DTU Library

Hyperspatial mapping of land surface water, energy and CO2 uxes from Unmanned Aerial Systems

Wang, Sheng

Publication date:
2019

Document Version
Publisher's PDF, also known as Version of record

Hyperspatial mapping of land surface water, energy and CO_2 fluxes from Unmanned Aerial Systems

Sheng Wang

PhD Thesis
January 2019

DTU Environment
Department of Environmental Engineering

Hyperspatial mapping of land surface water, energy and CO_2 fluxes from Unmanned Aerial Systems

Sheng Wang

PhD Thesis
January 2019

DTU Environment
Department of Environmental Engineering
Technical University of Denmark

PhD project: Hyperspatial mapping of water, energy and carbon fluxes with Unmanned Aerial Vehicles

Sheng Wang

PhD Thesis, January 2019

The synopsis part of this thesis is available as a pdf-file for download from the DTU research database ORBIT: http://www.orbit.dtu.dk.

Address:	DTU Environment Department of Environmental Engineering Technical University of Denmark Miljoevej, building 113 2800 Kgs. Lyngby Denmark
Phone reception:	+45 4525 1600
Fax:	+45 4593 2850
Homepage:	http://www.env.dtu.dk
E-mail:	reception@env.dtu.dk

Cover:	GraphicCo

Preface

The PhD thesis work "Hyperspatial mapping of land surface water, energy and CO_2 fluxes from Unmanned Aerial Systems" was conducted at the Department of Environmental Engineering at the Technical University of Denmark from October 2015 to January 2019 under the supervision of Associate Professor Monica Garcia and co-supervisors Professor Peter Bauer-Gottwein and Senior Scientist Andreas Ibrom. An internal PhD grant from the Department of Environmental Engineering at DTU is acknowledged for providing funding for this PhD project. Five scientific papers constitute the PhD work presented here. The papers are outlined below and will be referred to using the Roman numerals **I-V** throughout the thesis.

I **Wang**, **S.**, Baum, A., Zarco-Tejada, P., Dam-Hansen, C., Thorseth, A., Bauer-Gottwein P., Bandini F., & Garcia M. (2018) "Unmanned Aerial System multispectral mapping for low and variable solar irradiance conditions: potential of tensor decomposition". *Submitted.*

II **Wang, S**., Ibrom, A., Bauer-Gottwein, P., & Garcia, M. (2018). "Incorporating diffuse radiation into a light use efficiency and evapotranspiration model: An 11-year study in a high latitude deciduous forest". *Agricultural and Forest Meteorology*, 248, 479-493.

III **Wang**, **S.**, Garcia, M., Ibrom, A., Jakobsen, J., Josef Köppl, C., Mallick, K., Looms, M., & Bauer-Gottwein, P. (2018) "Mapping root zone soil moisture using a temperature-vegetation triangle approach with an Unmanned Aerial System: incorporating surface roughness from Structure-from-Motion". *Remote Sensing*, 10 (12), 1978.

IV **Wang**, **S.**, Garcia, M., Bauer-Gottwein, P., Jakobsen, J., Zarco-Tejada, P., Bandini, F., Sobejano Paz, V., & Ibrom, A. (2018) "High spatial resolution monitoring land surface energy, water and CO_2 fluxes from an unmanned aerial system". *Under review.*

V **Wang**, **S.**, Garcia, M., Ibrom, A., & Bauer-Gottwein, P. (2018) "Interpolating rapidly changing land surface energy, water and CO_2 fluxes between remote sensing acquisitions from an Unmanned Aerial System". *Manuscript.*

TEXT FOR WWW-VERSION (without papers)

In this online version of the thesis, paper **I-V** are not included but can be obtained from electronic article databases e.g. via www.orbit.dtu.dk or on request from DTU Environment, Technical University of Denmark, Miljoevej, Building 113, 2800 Kgs. Lyngby, Denmark, info@env.dtu.dk.

In addition, the following publications, not included in this thesis, were also parts of my PhD work:

Wang, S., van der Tol, C., Ibrom, A., Bayat, B., Yang, P., Bauer-Gottwein, P., Josef Köppl, C., Riedel, N., Dam-Hansen, C., & Garcia, M. (2018) "Coupled leaf-canopy and atmosphere radiative transfer modeling to evaluate the influence of aerosol optical depths on land surface CO_2 and water fluxes". *In preparation.*

Wang, S., Ibrom, A., Bauer-Gottwein, P., & Garcia, M. (2018) "Optimizing the revisit interval of remotely sensed observations for continuous estimation of rapidly changed land surface variables through the Bayesian analysis". *In preparation.*

Bandini, F., Lopez-Tamayo, A., Merediz-Alonso, G., Olesen, D., Jakobsen, J., **Wang, S**., Garcia, M., & Bauer-Gottwein, P. (2018). "Unmanned aerial vehicle observations of water surface elevation and bathymetry in the cenotes and lagoons of the Yucatan Peninsula, Mexico". *Hydrogeology Journal*, 1-16.

Bandini, F., Olesen, D., Jakobsen, J., Kittel, C. M. M., **Wang, S**., Garcia, M., & Bauer-Gottwein, P. (2018). "Bathymetry observations of inland water bodies using a tethered single-beam sonar controlled by an unmanned aerial vehicle". *Hydrology and Earth System Sciences*, 22(8), 4165-4181.

Christian, K., Bandini, F., **Wang, S**., Garcia, M., Bauer-Gottwein, P. (2016). Applying drones for thermal detection of contaminated groundwater influx (Grindsted Å). Appendix in Anvendelse af drone til termisk kortlægning af forureningsudstrømning. Report of Drone System (Henrik Grosen, Sune Nielsen), edited by Miljøstyrelsen.

Acknowledgements

This PhD project has been an amazing experience for me during the last three years. It could not be accomplished without great support, help and advice from my supervisors and many other people. I would like to express my sincere acknowledgement to all of you.

First of all, I owe my deepest gratitude to my supervisor Prof. Monica Garcia, for all of her guidance, advice, and encouragement throughout the past three years. I am deeply grateful for her to give me the opportunity to do my Ph.D. at DTU. Without her support and guidance, this research work could not have been possible. She is always generous in sharing her great knowledge and experience. She always provided me a lot of useful suggestions, when I got stuck. She always carefully revised my writing and provided useful feedback. She always encouraged and inspired me to explore interesting phenomena in nature. I really enjoyed the discussion with her to deepen into novel findings behind the data.

I would like to show my deep acknowledgement to my co-supervisor Prof. Peter Bauer-Gottwein. It has been almost six years since the first time I met Peter. Peter is a very nice person and always takes good care of his students. Peter has a very broad knowledge of different disciplines and he always gave me very useful suggestions. He always guided me into understanding the underlying principles, theories and equations, instead of superficial concepts. I really appreciate the meticulous instructions from him.

I would like to express my great appreciation to my co-supervisor Prof. Andreas Ibrom. Andreas is a very experienced and talented scientist. His rich data sets provided a solid foundation for this thesis work. With his great knowledge and strong experience in meteorology, ecology and climate sciences, Andreas always gave me constructive and impressive suggestions. I really liked his deductive way of thinking and reasoning.

I would also like to thank Dr. Jakob Jakobsen for teaching me how to fly drones, how to make payload and how to process GNSS data. He is a very friendly and kind person. He offered a great contribution to the technical part of drones. The DTU Space laboratory provided great facilities for me to do the technical work.

I also appreciate the help from all members of our UAV team, Filippo Bandini, Daniel Haugård Olesen, Gorka Mendiguren Gonzalez, Christian Josef Köppl, Veronica Sobejano Paz, Xiao Hu, Xin Liu, Emmanouil Tsitsigiannis and Hatem Ahmad Alaboud. Thanks a lot for your great contribution to the UAV platform and fieldwork. I would also like to thank for the invaluable friendship with you. I will always miss the moments with you in the field during nice Danish summers.

I also want to thank researchers at other DTU departments. Andreas Baum at DTU Compute provided great help on the tensor decomposition. Carsten Dam-Hansen, Anders Thorseth, Nicolas Riedel and Radu Malureanu at DTU Photonics offered support on sensor calibration and valuable irradiance data.

Furthermore, I would like to thank two hosts of my external stays. Prof. Pablo J. Zarco-Tejada gave me useful instructions on the sensor calibration. Prof. Christiaan van der Tol gave me many suggestions on the SCOPE modelling. I would also like to thank Prof. Bob Su, Alberto Hornero Luque, Peiqi Yang, Bagher Bayat, Jing Liu and other friends for their help during my external stay. It is pity that the SCOPE paper has been not be included in this thesis. I would also like to thank the financial support for my short-term scientific missions from the COST action OPTIMISE.

I would like also want to thank my other coauthors. Prof. Majken Looms at KU is always very friendly and I appreciated her help on the TDR instrument. Dr. Kaniska Mallick provided insightful suggestions on my manuscript.

My dear friends and colleagues at DTU environment, I could not finish this project without your help, encouragement and good company. My officemates Anne, Alex, Louise and Raphael always brought a lot of fun to the office. Prof. Dan Rosbjerg guided me in my first PhD conference in Vienna and my first conference during my master in Gothenburg. I would like to thank Prof. Kim Pilegaard as the PI of the flux sites and the head of our section. I also appreciate the help from PhD administration Anne and IT Hugo, Martin and Rene. Special thanks to Grith and Dan on the Danish summary of this thesis. I would also like to thank the internal funding from DTU, the smart UAV project and the AgWIT project to support my PhD.

I appreciate the guidance from Prof. Suxia Liu and Prof. Xingguo Mo at Chinese Academy of Sciences and Prof. Yanlian Zhou at Nanjing University!

Lastly, I would like to thank my family and friends outside DTU for their unconditional support!

Summary

The sustainable management of water resources and agricultural production is a key issue for socio-economic development. A first step to improve monitoring of water consumption, ecosystem production and water use efficiency of agricultural or natural ecosystems is to provide valuable and near-real time information to stakeholders. As an interdisciplinary approach, land surface modelling is an essential tool to quantify the coupled water, energy and CO_2 fluxes between the land surface and the atmosphere, e.g. net radiation (Rn), soil moisture, evapotranspiration (ET) and gross primary productivity (GPP). Unmanned aerial systems (UAS) can provide remotely sensed imagery of ecosystems at very high spatial resolution (meter level) with low cost and flexible revisit times regardless of cloudy conditions, which can be incorporated into land surface models. However, there remain challenges for operational monitoring of land surface fluxes from UAS, especially in northern latitudes: the limited payload capacity (< 2kg) of most commercial UAS, low signal-to-noise ratios of miniaturized sensors, the frequent cloudy weather, the lack of ad-hoc operational methodologies to estimate fluxes, implications of flying under overcast conditions, or temporal gaps in fluxes between the image acquisitions.

This thesis aims to design an operational UAS monitoring system to estimate land surface fluxes by integrating land surface models and UAS imagery. Specifically, the thesis addresses the following questions:

(Objective 1) Can high quality reflectance and thermal imagery be obtained from UAS for quantitative remote sensing research? What kind of accuracy can be achieved for UAS imagery obtained in low and variable irradiance?

(Objective 2) Can the high spatial resolution of land surface water, energy and CO_2 fluxes be mapped from UAS imagery? What controls the spatial variability of land surface fluxes?

(Objective 3) Can UAS based instantaneous estimates of fluxes be temporally upscaled to the continuous daily values? Is there any important environmental factor to influence the temporal dynamics of land surface fluxes at the considered ecosystem?

To achieve these objectives, UAS optical and thermal imagery and eddy covariance observations were integrated with ‘top-down’ operational land surface models, which quantify ET and GPP with joint environmental constraints. Case studies were mainly conducted in a Danish willow bioenergy forest eddy

covariance site (DK-RCW), while the long-term eddy covariance observations from a deciduous beech forest eddy covariance site (DK-Sor) were used for model development. The thesis includes three main parts to address each of the three objectives stated above.

Sensor calibration and image processing: With thorough laboratory sensor calibration for low illumination and application of the improved image processing procedures, the potential of UAS multispectral mapping in low and variable irradiance conditions of northern latitudes was exploited. Particularly, a four-way Tucker tensor decomposition method was used to remove the cloud shadow in UAS imagery. Outdoor experiments indicate that the multispectral imagery can provide reliable reflectance with root mean square deviations (RMSDs) around 3%. This shows the potential of UAS mapping for quantitative Remote sensing research.

Spatial variability of land surface fluxes: A simple but operational 'top-down' ET and GPP snapshot model, which jointly estimates evapotranspiration and carbon assimilation with the same environmental constraints, was developed (Wang et al., **II**). To provide soil moisture constraints for ET simulation, the root-zone soil moisture from UAS optical and thermal imagery was estimated by the modified temperature-vegetation triangle approach at DK-RCW showing the benefits of incorporating tree height from the Structure-from-Motion (SfM) (Wang et al., **III**). Furthermore, high spatial resolution of Rn, ET and GPP at the time of flights was estimated with the 'top-down' snapshot model (Wang et al., **IV**). Compared to the source-weighted footprint, the case study at DK-RCW shows that this joint model with UAS optical and thermal imagery can well estimate ET, GPP, and water use efficiency with RMSDs equal to 41.2 $W \cdot m^{-2}$, 3.12 $\mu mol \cdot C \cdot m^{-2} \cdot s^{-1}$, and 0.35 $g \cdot C \cdot kg^{-1}$, respectively. Our spatial scale analyses stressed the importance to consider the heterogeneity within the eddy covariance footprint, as the model performance degraded with coarser spatial resolution. By using the semivariogram and an experiment aggregating model inputs into different spatial resolutions, it was found that imagery resolution consistent with the tree crown size (1.5 m in our case) was sufficient to capture the spatial heterogeneity of the fluxes. Our results highlight the importance of considering the heterogeneity of land surface for flux modeling and the source contribution within the eddy covariance footprint for model benchmarking at appropriate spatial resolutions.

Temporal variability of land surface fluxes: In the temporal upscaling from the instantaneous to the diurnal, it was found that it is important to consider the change of eddy covariance footprints during the course of the day for model benchmarking with eddy covariance observations (Wang et al., **IV**). To temporally interpolate the flux estimates between days without UAS data acquisitions, a dynamic Soil-Vegetation, Energy, water and CO_2 traNsfer model (SVEN) was developed (Wang et al., **V**). Based on instantaneous estimates (Wang et al., **IV**), this model can accurately provide continuous estimates of land surface fluxes. This provides a methodology to temporally upscale the remote sensing based instantaneous estimates into daily or longer time scales. Furthermore, with 11-year long-term eddy covariance observations, Wang et al. (**II**) analysed the independent and joint effects from diffuse radiation on the temporal variability of GPP and ET. In this Danish ecosystem, diffuse radiation plays a crucial role to enhance ecosystem light use efficiency and water use efficiency.

This UAS based monitoring system can be valuable for applications in agricultural and water resources management, and it would also be beneficial for scientific communities, e.g. remote sensing, ecohydrology and micrometeorology, to identify processes at high spatial resolution. Additionally, this system requires limited ground observations and can be applied for routine monitoring applications in data-scarce regions.

Dansk sammenfatning

Bæredygtig forvaltning af vandressourcer og landbrugsproduktion er afgørende for socioøkonomisk udvikling. Først og fremmest skal overvågningen af vandforbrug, økosystemproduktion og udnyttelsen af vandressourcer i landbrugs- eller naturlige økosystemer forbedres for at opnå data tæt på realtidsinformation. Landoverflade-modellering er et væsentligt redskab til at kvantificere koblede vand-, energi- og CO_2-fluxe mellem landoverfladen og atmosfæren, f.eks. nettostråling (Rn), jordfugtighed, evapotranspiration (ET) og brutto-primærproduktivitet (GPP). Til anvendelse i landoverflademodeller kan ubemandede luftfartøjer (UAS) tilvejebringe remote sensing billeder af økosystemer med meget høj rumlig opløsning (meter-niveau) med lave omkostninger og fleksible tidsrum mellem observationer uanset overskyede forhold. Imidlertid er der stadig en lang række udfordringer for operationel monitering af landoverflade-fluxe med UAS, især på de nordlige breddegrader: den begrænsede nyttelastkapacitet (<2 kg) af de fleste kommercielle UAS, den lave ratio mellem signal og støj for minisensorer, det hyppigt overskyede vejr, manglen på ad hoc-operationelle metoder til at estimere flux, konsekvenser af flyvning under overskyede forhold og tidsmæssige huller i flux mellem billeddata-optagelser.

Formålet med denne afhandling er at designe et operationelt UAS-overvågningssystem til vurdering af landoverfladeflux ved at integrere landoverflademodeller og UAS-billeder. Afhandlingen har specielt fokus på følgende spørgsmål:

(Formål 1) Kan der opnås højkvalitets-reflektans og termisk billeddannelse fra UAS til kvantitativ remote sensing forskning? Hvilken slags nøjagtighed kan opnås for UAS-billeder opnået i lav og variabel bestråling?

(Formål 2) Kan den høje rumlige opløsning af overfladevand, energi og CO_2-fluxe kortlægges fra UAS-billeder? Hvad styrer rumlig variation af fluxe fra jordoverfladen?

(Formål 3) Kan UAS-baserede øjeblikkelige estimater af fluxe opskaleres midlertidigt til løbende daglige værdier? Er der nogen vigtig miljøfaktor, der påvirker den tidsmæssige dynamik af overflade-fluxe i det betragtede økosystem?

For at nå ovenstående målsætninger blev optiske og termiske UAS billeder og eddy covariance observationer integreret med 'top-down' operationelle landoverflade-modeller, som kvantificerer ET og GPP med fælles miljømæssige

begrænsninger. Case-studierne blev primært udført på en dansk energi-pileskov (DK-RCW), mens de længerevarende eddy covariance observationer fra en dansk løvskov (DK-Sor) blev anvendt til modeludvikling. Afhandlingen indeholder tre hoveddele, der hver behandler et af de tre ovennævnte formål.

Sensorkalibrering og billedbehandling: Med en grundig laboratoriesensorkalibrering til den lave indstrålingsintensitet og de forbedrede billedbehandlingsprocedurer blev potentialet ved UAS multispektral kortlægning undersøgt for lave og variable strålingsforhold gældende for nordlige breddegrader. Især blev en four-way Tucker tensor dekompositions-metode brugt til at fjerne skyggen fra skyer i UAS billeder. Udendørs eksperimenter indikerer, at multispektrale billeder kan give pålidelig refleksion med root mean square afvigelser (RMSD) omkring 3%. Dette viser potentialet for brugen af UAS-kortlægning i kvantitativ remote sensing forskning.

Rumlige variationer af jordoverfladeflux: En simpel men operationel 'top-down' ET og GPP snapshot model, der samlet vurderer evapotranspiration og carbon-assimilering med samme miljømæssige begrænsninger, blev udviklet (Wang et al., **II**). For at tilvejebringe jordfugtigheds-grænser for ET-simulering blev jordzonefugtigheden fra UAS-optiske og termiske billeder estimeret ved den modificerede temperatur-vegetation triangulerings-metode i DK-RCW, hvilket viste fordelen ved at inkludere træhøjde fra Structure-from-Motion (SfM) (Wang et al., **III**). Desuden blev den høje rumlige opløsning af Rn, ET og GPP på tidspunktet for flyvninger anslået med 'top-down'-snapshot-modellen (Wang et al. **IV**). Sammenlignet med et kildevægtet footprint viser casestudiet på DK-RCW, at den integrerede model med optiske og termiske UAS billeder kan estimere ET, GPP og udnyttelsen af vand med RMSD'er svarende til 41,2 $W \cdot m^{-2}$, 3,12 $\mu mol \cdot C \cdot m^{-2} \cdot s^{-1}$ og 0,35 $g \cdot C \cdot kg^{-1}$. Vores rumlige skalaanalyser viste betydningen af at tage heterogeniteten af eddy covariance footprints i betragtning, da modellens ydeevne blev forringet med en grovere rumlig opløsning. Ved at anvende semi-variogrammet og et eksperiment, der aggregerer modelindgange i forskellige rumlige opløsninger, blev det fundet, at billedopløsningen i overensstemmelse med trækronens størrelse (1,5 m i vores tilfælde) var tilstrækkelig til at fange fluxenes rumlige heterogenitet. Vores resultater fremhæver vigtigheden af at medtage heterogeniteten af landoverfladen til fluxmodellering og kildebidraget i eddy covarinace footprints til model-benchmarking med passende rumlige opløsninger.

Tidsvariabilitet af landoverfladeflux: I den tidsmæssige opskalering fra det øjeblikkelige til daglige værdier blev det fundet, at det er vigtigt at medtage ændringen af eddy covariance footprints i løbet af dagen til model-benchmarking med eddy covariance observationer (Wang et al., **IV**). For temporært at interpolere flux estimaterne mellem dage uden UAS data opkøb blev der udviklet en dynamisk Soil-Vegetation, Energy, Water og CO_2 traNsfer model (SVEN) (Wang et al., **V**). Baseret på snapshot estimater (Wang et al., **IV**) kan denne model give nøjagtige, kontinuerlige estimater af landoverflade-flux. Hermed opnås en metode til at opskalere remote sensing snapshot målinger til daglige eller længere tidsskalaer. Endvidere analyserede Wang et al. (**II)** de uafhængige og fælles effekter fra diffus stråling på den tidsmæssige variabilitet af GPP og ET ved udnyttelse af 11 års eddy covariance observationer. I det betragtede danske økosystem spiller diffus stråling en afgørende rolle for at forbedre økosystemets indstrålings-effektivitet og effektiviteten af vandforbruget.

Dette UAS-baserede overvågningssystem kan være værdifuldt for applikationer inden for forvaltning af landbrug og vandressourcer, og det ville også være til gavn for videnskabelige grene som f.eks. for remote sensing, økohydrologi og micro-meteorology til at identificere processer ved høj rumlig opløsning. Systemet kræver begrænsede landobservationer og kan anvendes til rutinemæssige overvågninger og i områder med dataknaphed.

Table of contents

Abbreviations

CI	Cloudiness Index
DSM	Digital Surface Model
ET	Evapotranspiration
λLE	Latent Heat Flux
GCPs	Ground Control Points
GNSS	Global Navigation Satellite System
GPP	Gross Primary Productivity
GPS	Global Positioning System
IMU	Inertial Measurement Unit
LAI	Leaf Area Index
LUE	Light Use Efficiency
mamsl	Meters Above Mean Sea Level
NDVI	Normalized Difference Vegetation Index
NIR	Near Infrared
PAR	Photosynthetically active radiation
PPK	Post Processing Kinematic
RGB	Red Blue Green
RH	Relative Humidity
RMSD	Root Mean Square Deviation
Rn	Net Radiation
RTK	Real Time Kinematic
SBC	Single Board Computer
SfM	Structure-from-Motion
SM	Soil Moisture
T_s	Land Surface Temperature
UAS	Unmanned Aerial System
UAV	Unmanned Aerial Vehicle
VHR	Very High spatial Resolution
VPD	Vapour Pressure Deficit
VTOL	Vertical Take-Off and Landing
WUE	Water Use Efficiency

1 Introduction

1.1 Background and motivation

The sustainable management of water resources and food production is a key issue for the socio-economic development. During the past 50 years, water consumption has tripled and agriculture consumes two thirds of world water resources (Gilbert, 2012). Due to global climate change and growing population, the pressure on water and food security is going to increase in the next 50 years. Based on global climate projections, the future global agricultural water consumption will increase around 20% by 2050 (Wada and Bierkens, 2014). The first step to achieve sustainable management starts by quantifying the use of water and carbon assimilation by terrestrial ecosystems continuously in space and time. Particularly, the high spatial resolution metrics on water use and carbon assimilation have the potential to inform policy makers, conservation agencies, farmers and agribusinesses to detect the early stressed patches to take adaptive management to avoid damage to a larger scale.

The precise impact of climate changes and extreme events on ecosystems remains largely unknown, due to knowledge gaps on the joint regulation of water and carbon fluxes between the varieties of interplayed processes. Modeling schemes should aim at unifying the coupled ET, carbon and energy budgets (Fisher et al., 2017). Land surface modelling, which aims at quantitatively estimate coupled energy, water and carbon fluxes between terrestrial ecosystems and the atmosphere, has emerged as an interdisciplinary from hydrology, meteorology, ecology and remote sensing communities. It is a useful tool to for scientists to quantify the coupled energy, water and carbon budgets, but also policy makers to evaluate policies to mitigate the climate change effects. The core of land surface modelling focuses on quantifying interactions among vegetation carbon assimilation, energy and water. Vegetation is a highly dynamic component of the Earth system and plays a vital role in regulation of the surface-atmosphere flux exchanges, with photosynthesis converting light, water and CO_2 into sugar and oxygen. During the past decades, Earth observation (EO) techniques offer rich data sources to monitor vegetation dynamics in a large scale. For instance, satellite remote sensing data have been used as inputs or parameters to significantly improve the land surface modelling. However, our understanding of land surface energy, water and carbon dynamics is limited by the coarse spatial resolutions of current land surface modelling schemes, which cannot represent the spatial heterogeneity in topography, soils, and vegetation (Wood et al., 2011).

With progress on the platform stability, reliability and flexibility, Unmanned aerial systems (UAS), commonly known as drones, Unmanned Aerial Vehicles (UAV) or Remotely Piloted Aircraft Systems (RPAS), deployed with miniaturized imaging sensors can provide timely remote sensing imagery of ecosystems at very high spatial resolution (VHR, meter level). The VHR imagery from UAS presents an unprecedented opportunity to provide for hyper-resolution land surface characterizations, monitoring, modelling and predictions (Vivoni et al., 2014). With UAS remote sensing imagery, ecohydrological variables as evapotranspiration (ET) and gross primary productivity (GPP), or crop yields can be accurately quantified at VHR. This is of great potential for the sustainable water resources and ecosystem management.

Compared satellite-based observations, UAS can provide VHR imagery with flexible revisit time and low cost. The combination of VHR UAS data and land surface modelling has the following merits: First, the high-resolution spatial data can fill the scale discrepancy between satellite imagery and field measurements. Traditionally, most of land surface modelling using satellite-based data operate at spatial resolutions of 40km, if coupled to climatological models (online), or around 1-3 km, in off-line approaches (Anderson et al., 2011). Land surface modelling at such coarse resolution involves uncertainties in mixture of land cover types within the pixel and in model benchmarking with field measurements (Lipton et al., 2015). However, UAS bring remote sensing (RS) observations into a sub-meter level and the imagery will mainly consist of pure pixels (only one land cover type inside). This is beneficial to detect the spectral change of the land cover, especially for vegetation. Besides the high spatial resolution, new types of spectral information from UAS can be incorporated into land surface models via data assimilation or directly as model forcing. The combination of thermal and optical sensors such as hyper-spectral and multi-spectral images can be used to retrieve several key land surface variables or parameters, e.g. vegetation indices, surface albedo, radiometric temperature, emissivity, spectral indicators of light use efficiency and photosynthesis, canopy water content and near surface soil moisture (Clevers and Kooistra, 2012; Sims et al., 2006). They can improve the current capabilities of land surface modelling, in which prescribed leaf area index or albedo are routinely used (e.g. Community Land Surface model, Lawrence et al., 2011). Other advantages of UAS compared to satellites are their flexible turnaround times and the capability of flying in cloudy conditions. This makes them applicable in precision agriculture, wildfire detection, flood and glacier monitoring (Berni et al., 2009; Colomina and Molina, 2014). Additionally, the operating costs of UAS are lower compared to manned airborne surveys or satellite observations. This offers new opportunities for scientists and companies, and promotes the flexible UAS based remote sensing applications around the world.

1.2 Research objectives

This main objective of this PhD thesis is to design an operational UAS based monitoring system to map the land surface water, energy and CO_2 fluxes including net radiation, soil moisture, ET and GPP with high spatial resolution. Specific objectives are addressed below as questions:

(Objective 1) Can high quality reflectance and thermal imagery be obtained from UAS for quantitative remote sensing research? What kind of accuracy can be achieved for UAS imagery obtained in low and variable irradiance?

(Objective 2) Can the high spatial resolution of land surface water, energy and CO_2 fluxes be mapped from UAS imagery? What controls the spatial variability of land surface fluxes?

(Objective 3) Can UAS based instantaneous estimates of fluxes be temporally upscaled to the continuous daily values? Is there any important environmental factor to influence the temporal dynamics of land surface fluxes at this ecosystem?

1.3 Thesis structure

To achieve these objectives, this thesis has following content:

1. Sensor calibration and image processing: Conduct thoroughly calibration of the UAS imaging sensors and improve UAS image processing procedures, e.g. cloud shadow removal, for low and variable irradiance conditions in northern high latitudes (Wang et al., **I**).

2. Spatial variability of land surface fluxes: Develop a joint ‘top-down’ ET and GPP snapshot model to estimate land surface fluxes (Wang et al., **II**). To provide the soil moisture constraint for ET, the root-zone soil moisture from UAS optical and thermal imagery was estimated by the modified temperature-vegetation triangle approach with showing benefits of incorporating tree height from the Structure-from-Motion (SfM) (Wang et al. **III**).

Furthermore, Wang et al., (**IV**) estimated the spatial variability of Rn, ET and GPP at the time of flights, assessed the optimum spatial resolution to benchmark models with eddy covariance observations, and identified the major factor to control the spatial variability of land surface fluxes in the study site.

3. Temporal variability of land surface fluxes: Wang et al. (**IV**) shows the approach to upscale the UAS based instantaneous estimates to the diurnal estimates. Further, a temporal dynamic model was developed to interpolate the flux estimates between UAS data acquisitions (Wang et al., **V**). Additionally, Wang et al. (**II**) analysed the independent and joint effects from diffuse radiation to the temporal variability of GPP and ET with 11-year long-term eddy covariance observations and included the effect of diffuse light in the modelling framework.

This synopsis is structured in seven chapters. The first chapter introduces the motivation and objectives of this thesis. The second chapter briefly summarizes the state-of-the-art UAS remote sensing techniques, the monitoring and modelling approaches on land surface water, energy and CO_2 fluxes, and the model-data integration.

Successively, the chapter on the study sites describes the climate and environmental conditions for the study sites. Then, the materials and methods section summarize the UAS platform and sensors, in-situ measurements, UAS image processing techniques and modelling approaches. This chapter also shows the approach to incorporate VHR remote sensing imagery from UAS into 'top-down' land surface models to estimate land surface fluxes spatially and temporally.

The results section highlights the scientific achievements of the research objectives (belonging to five scientific papers) demonstrating the benefits of using UAS remote sensing techniques for monitoring land surface fluxes. Detailed connections among five scientific papers are summarized in Figure 1-1.

In conclusion and future perspectives, the potential applications of this UAS monitoring system and future improvements for monitoring land surface fluxes are discussed.

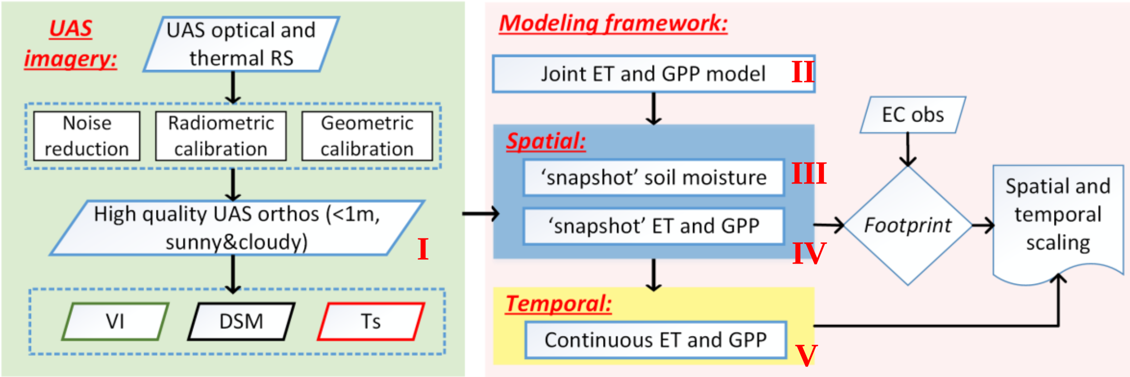

Figure 1-1. Graphic abstract of this thesis. The roman number corresponds to each scientific paper. *UAS imagery*: an imaging payload consisting of a six band multispectral camera, a thermal infrared camera and a normal Red-Green-Blue channel camera was deployed on a hexacopter to conduct flight campaigns at an eddy covariance site DK-RCW. With radiometric and geometric correction and noise reduction, the UAS imagery was processed into high-quality orthophotos (Wang et al. **I**). The modelling framework includes three parts, the development of the joint ET and GPP model (Wang et al., **II**), the simulation of the spatial variability of land surface fluxes, and the simulation of the temporal variability of land surface fluxes. *Spatial*: UAS based vegetation index (VI), surface temperature (T_s) and digital surface elevation model (DSM) were further used as inputs of the modified temperature-vegetation triangle approach to estimate soil moisture (Wang et al., **III**), and later as inputs of the joint ET and GPP model to simulate net radiation, evapotranspiration (ET) and gross primary productivity (GPP) (Wang et al., **IV**). These simulated land surface fluxes were validated with the eddy covariance (EC) observations and explore spatial scaling issues. *Temporal*: to interpolate the snapshot estimates, the UAS data were used as inputs of the dynamic 'SVEN' model to continuously estimate ET and GPP (Wang et al., **V**).

2 Background

2.1 Unmanned aerial system based remote sensing of land surface fluxes

Remote sensing is a technique to acquire information about an object based on the reflected or emitted electromagnetic or gravitational signals without any physical contact (Sanderson, 2010). Remote sensing is an essential approach to monitor land surface conditions to provide various spatial, temporal and spectral information. Based on the platform, remote sensing can be classified into satellite, manned and unmanned airborne techniques. As an emerging field, UAS are highlighted to offer unprecedented opportunities in ecological and environmental monitoring (Anderson and Gaston, 2013), particularly in the context of precision agriculture (Zarco-Tejada et al., 2012). The UAS remote sensing technique is acknowledged as one of the most exciting recent advances in near-Earth observation (McCabe et al., 2017). From the number of publication, as shown in Figure 2-1, there is a rapid growing trend for the UAS application in environmental monitoring, especially during the last five years (Manfreda et al., 2018).

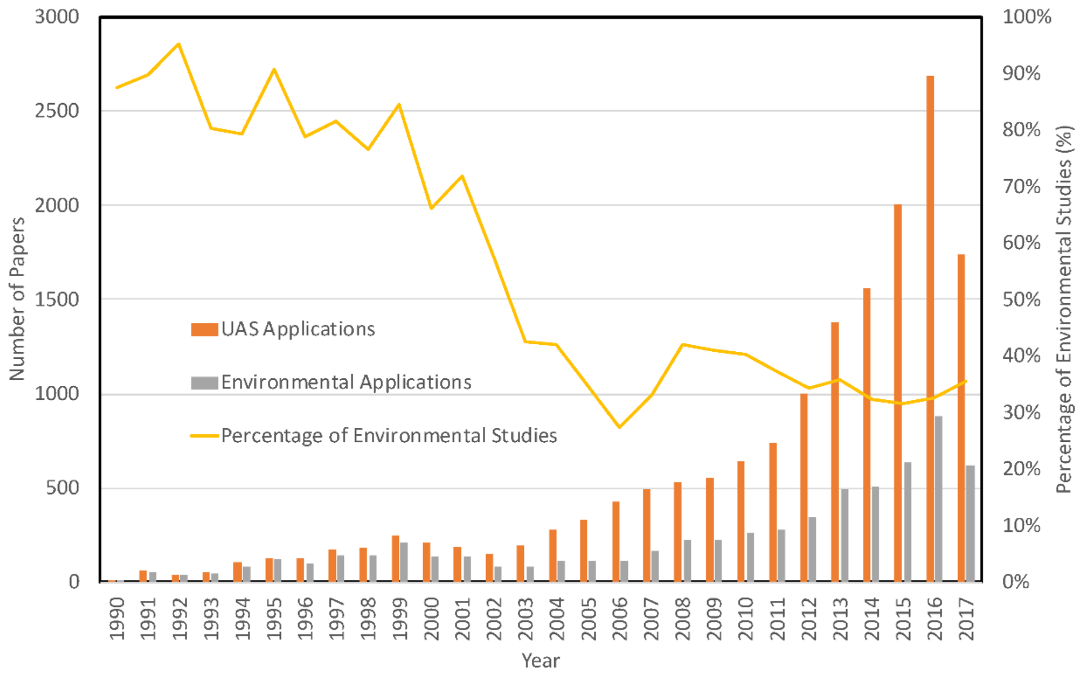

Figure 2-1. Number of articles extracted from the database ISI-web of knowledge published from 1990 up to 2017 (last access 15 January 2018). (Manfreda et al., 2018)

Compared to satellites or manned airborne systems, UAS are affordable, can be operated autonomously and offer exceptional spatial resolution for observing the land surface. In addition, UAS have the potential to be deployed rapidly and repeatedly to acquire high spatial and temporal resolution data with legislation and permits being the most limiting factor for operational approaches. The VHR imagery from UAS can fill the gaps between satellites and tower based remote sensing to facilitate our understanding towards the scaling issues (Anderson and Gaston, 2013; Klosterman et al., 2018). Moreover, UAS flight campaigns can be conducted under various weather conditions. This enables to collect optical and thermal imagery under cloudy weather conditions, while satellites in optical and thermal domains cannot provide observations of the land surface. This is particularly important for high latitudes e.g. Denmark, where cloudy days are frequent (Wang et al., 2018a). Low operation cost is also an advantage of UAS remote sensing techniques.

The flexibility to deploy various sensors is another advantage of UAS remote sensing. Ideally, all kinds of satellite remote sensing techniques and methods can be applied with UAS but they also require adaptation (Wang et al., 2018b). However, with limitation of the payload weight capacity, the most common used UAS remote sensing techniques are RGB (Red-Green-Blue channel), multispectral, hyperspectral, thermal imaging and LiDAR (light detection and ranging techniques) as shown in Figure 2-2. These remote sensing techniques including optical, sun induced fluorescence (SIF), thermal and LiDAR data have their own unique but also shared values for vegetation status monitoring (Guan et al., 2016). For instance, reflectance, SIF, thermal and LiDAR data can be utilized to analyse the vegetation water stress. However, as shown in Figure 2-2, different techniques reflect the drought stress in different stages and time scales. SIF directly links with the photosynthesis rate and can be an early stress indicator (Guanter et al., 2014). The thermal infrared signals reflect the transpiration rate of vegetation and the photochemical reflectance index indicates the photosynthesis at short time scales. Both of them can be used as indicators of early stage stress (Zarco-Tejada et al., 2013). With more severe drought, the leaf water content, leaf inclination angles and pigments will change. At this late stage, the stress can be detected by changes in reflectance using the UAS multispectral or hyperspectral techniques. Further, the drought induces senescence and deciduousness in the canopy. UAS based LiDAR techniques can be applied to monitor the change of leaf area index and vegetation morphology.

In this thesis, UAS based thermal and multispectral techniques were utilized to detect vegetation status and further to estimate land surface fluxes.

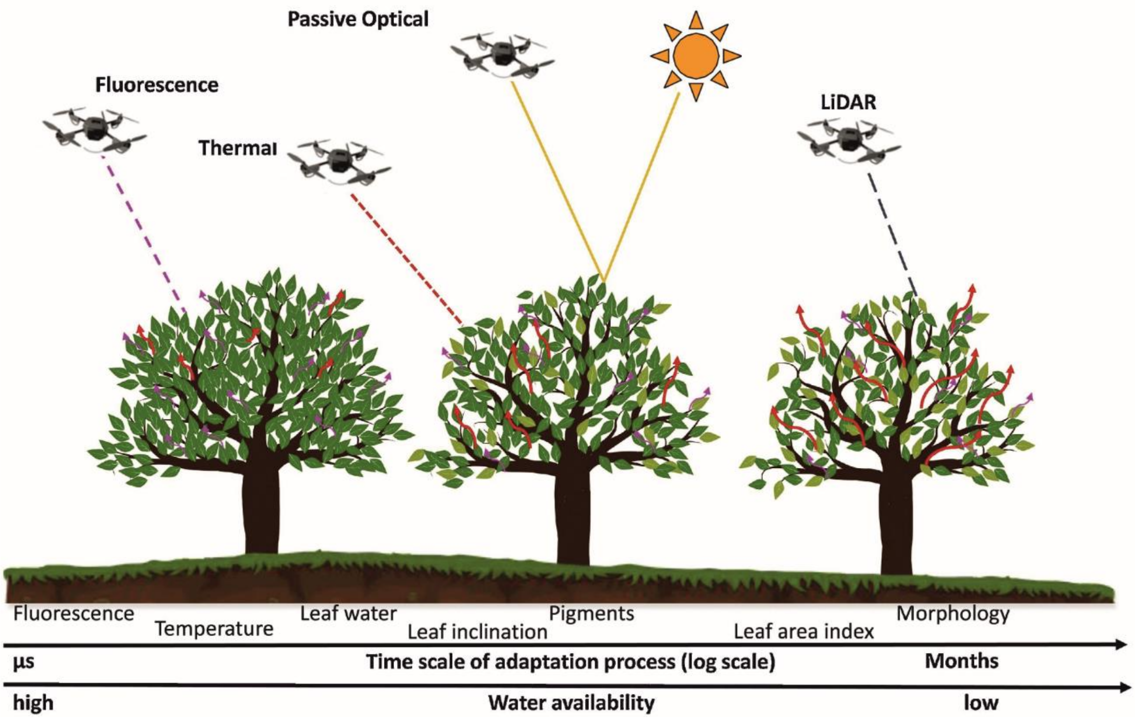

Figure 2-2. Overview of various UAS based remote sensing techniques for detecting the physiological, biochemical, and structural responses of vegetation to the water stress. Purple arrows and lines indicate fluorescence radiation emitted by plants. Red arrows and lines relate to thermal radiation emission. The yellow lines represent the reflected solar spectrum while the green lines indicate the reflected LiDAR signals. Sun induced fluorescence (SIF), thermal radiation, reflectance and LiDAR signals obtained from UAS can be used to detect different levels of vegetation water stress and the corresponding adaptation processes in different time scales. (Adapted from Damm et al., 2018)

UAS based remote sensing has been widely applied for various environmental monitoring applications, such as vegetation height (e.g. Zarco-Tejada et al., 2014), vegetation species classification (e.g. Laliberte et al., 2011), vegetation biophysical parameters (e.g. Berni et al., 2009) and vegetation water stress (e.g. Zarco-Tejada et al., 2013). Anderson and Gaston (2013) highlighted that the VHR imagery can improve our understanding on the land surface-atmosphere interactions. However, studies on using UAS for monitoring land surface fluxes are rare.

Regarding soil moisture, Hassan-Esfahani et al. (2015, 2017) used the artificial neural network to estimate the spatial variability of soil moisture from UAS optical and thermal imagery. Results indicated that a good accuracy with root mean square deviations (RMSDs) equal to 0.05 $m^3 \cdot m^{-3}$ can be achieved. Wang et al. (2018) used the water deficit index (Moran et al., 1994) to quantify soil moisture in experimental plots of spring wheat (Wang et al., 2018c) and achieved a good accuracy with a coefficient of determination (R^2) of 0.63 and RMSDs less than 0.10 $m^3 \cdot m^{-3}$.

For ET, recent studies demonstrated that UAS thermal imagery incorporated to the Two Source Energy Balance (TSEB) model (Kustas and Norman, 1999) can estimate ET with RMSDs around 10-30% of the measured fluxes over irrigated crops (Hoffmann et al., 2016; Kustas et al., 2018; Ortega-Farías et al., 2016) and grasslands (Brenner et al., 2017). For GPP, Zarco-Tejada et al. (2013) demonstrated chlorophyll fluorescence, physiological indices (e.g. photochemical reflectance index, PRI), and structural indices (e.g. normalized difference vegetation index, NDVI) and enhanced vegetation index derived from UAS observations correlate well with the measurements of CO_2 fluxes from the eddy covariance.

2.2 Eddy covariance technique

Emerging from micrometeorology, the eddy covariance technique has been widely applied across different ecosystems and climate regions around the world to measure flux exchanges e.g. heat, water vapour or trace gasses (CO_2 or methane) between the land surface and the atmosphere (Baldocchi, 2003). It has been increasingly used to interpret the ecohydrological processes or to benchmark land surface models (Jung et al., 2011).

In terms of terrestrial ecology, eddy covariance measurements are often conducted with a tower installed within the atmospheric surface boundary layer, seen as Figure 2-3A. The atmospheric airflow that surrounds the tower is by turbulences and can be visualized as a general horizontal flow comprised of rotating eddies (Metzger, 2018). Eddies facilitate the upwards and downwards transport of the land surface fluxes, seen as Figure 2-3B. The net flux exchanges depends on the covariance between the vertical transport velocity facilitated by the eddies (momentum transport) and the concentration of the tracer gases transported (Kljun et al., 2015).

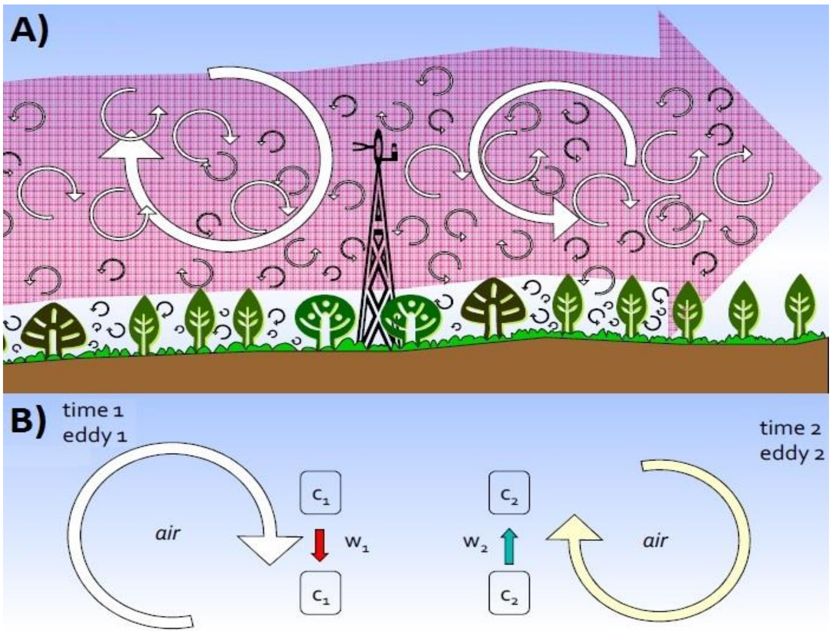

Figure 2-3. The overview of eddy covariance techniques. (Burba, G., 2013. Eddy Covariance Method for Scientific, Industrial, Agricultural and Regulatory Applications: a Field Book on Measuring Ecosystem Gas Exchange and Areal Emission Rates. LI-COR Biosciences, Lincoln, USA, 331 pp.)

The eddy covariance flux tower networks have been widely implemented at the global scale to measure the exchange of water vapour, energy and CO_2 fluxes between the terrestrial ecosystems and the atmosphere, e.g. Integrated Carbon Observatory System (ICOS, www.icosinfrastructure.eu) in Europe, National Ecosystem Observatory Network (NEON, www.neonscience.org) in USA, AsiaFlux in Asia (http://www.asiaflux.net/), and global FLUXNET (www.fluxnet.ornl.gov). The main function of FLUXNET is to provide data series for i.e. carbon fluxes alongside with auxiliary outputs of energy and water fluxes for data interpretation (Baldocchi, 2003). The data can be independently used to integrate the ecohydrological processes and also can be integrated with models as model inputs or parameters (Running et al., 1999).

In this thesis, the eddy covariance measurements were used for model benchmark to test the accuracy of the designed UAS monitoring system for estimation of land surface water, energy and CO_2 fluxes. On the other hand, the VHR imagery from this UAS monitoring system can provide insights into the heterogeneity of the eddy covariance footprint. This can facilitate our understanding on the scaling issues and energy closure issues for the eddy covariance system (see Figure 1-1 integration part).

2.3 Land surface modelling

The modelling of atmosphere-land exchange processes, i.e. the energy, water and CO_2 flux exchanges between the land surface and the atmosphere, across a range of spatial and temporal scales can improve our understanding of ecosystem functioning. Quantification of land surface fluxes is also important for the establishment of regional and global carbon budgets for climate change mitigation. It also has great benefits for local applications, e.g. precision agriculture.

Land surface modelling can be broadly classified into two categories (Houborg et al., 2009), 'top-down' and 'bottom-up' approaches. The 'top-down' approach neglects the behaviour of individual leaves and considers the effective canopy response to its environment as a bulk. 'Top-down' approaches estimate the potential functioning of canopy in terms of water and carbon fluxes under ideal conditions, and then down-regulate the functioning from this potential state into the actual value by considering the effect of various environmental constraints (García et al., 2013; Houborg et al., 2009). On the contrary, 'bottom-up' approaches provide detailed mechanistic descriptions of leaf-level photosynthetic processes, which are then upscaled to the canopy level. The 'top-down' method is similar to what has been referred in hydrology as a Darwinian approach, more concerned with explaining the ecological behaviour of systems (e.g. watersheds or canopies) as a whole and identifying processes by analysis of the statistical relationship between environmental constraints and surface fluxes as in Budyko approaches (Farmer et al., 2003; Zhang et al., 2008). While the 'bottom-up' method can be considered as part of what in hydrology has been referred to as a Newtonian modelling approach, where the detailed physical mechanisms are explicitly described at all spatial scales (Sivapalan et al., 2003).

The 'top-down' ET and GPP models treat the canopy/soil (or pixel) as a bulk and are generally less complex. The potential GPP or ET is constrained by various empirical relationships describing environmental stressors (e.g. temperature, soil moisture). This 'top-down' approach is capable to incorporate various remote sensing information to describe these environmental stressors (García et al., 2013; Houborg et al., 2009). One of the 'top-down' GPP model examples is the light use efficiency (LUE) approach, as shown in Figure 2-4. It is based on the assumption that plants adjust their growth to optimize resource acquisition of light and water (Fisher et al., 2008; García et al., 2013;

Nemani and Running, 1989). The representation of the 'top-down' model variables can be directly connected to remote sensing observations. For instance, GPP can be directly linked to SIF (Guanter et al., 2014). The fraction of the absorbed PAR can be estimated from vegetation indices e.g. normalized vegetation difference index (NDVI) (Wang et al., 2018a). The actual light use efficiency (ε) can be assessed by photochemical reflectance index (PRI) and fluorescence yield (Garbulsky et al., 2011; van der Tol et al., 2009). Similar to the LUE approach to estimate carbon assimilation, ET can also be calculated through the 'top-down' approach, for example Priestley-Taylor Jet Propulsion Laboratory ET model (PT-JPL, Fisher et al., 2008). The PT-JPL model first estimates the potential ET with the Priestley-Taylor equation. Then the model down regulates the potential ET to the actual one by various remote sensing and meteorological observations reflecting the environmental constraints of vegetation and soil, such as NDVI, soil adjusted vegetation index (SAVI), enhanced vegetation index (EVI) or air temperature.

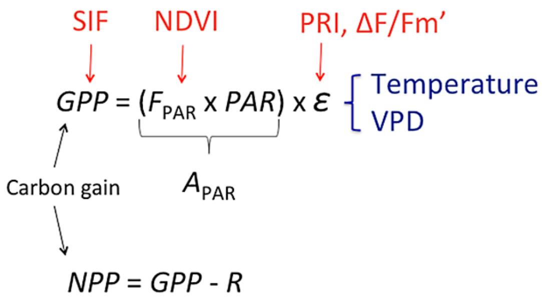

Figure 2-4. Representation of the LUE model, showing optical measurements useful for model parameterization and validation (red text), including solar induced fluorescence, NDVI, PRI and fluorescence yield. Alternatively, light efficiency (ε) can be addressed using meteorological data (temperature and vapor pressure deficit) or thermal remote sensing and modeling methods (Gamon, 2015).

Land surface modelling intended for routine applications should attempt to balance computation demands and the capability for simulating the responses of CO_2, water, and energy fluxes to environmental and physiological forcing. As the 'top-down' approach is simple but operational, it can be routinely applied to monitor the land surface fluxes. For instance, the MODIS products using the LUE approaches can provide global estimates of GPP every 8 day (Running et al., 2004). Thus, the 'top-down' approach is adopted in this thesis to combine with UAS imagery for monitoring land surface fluxes.

3 Study sites and in-situ measurements

This study was conducted in two Danish eddy covariance sites. One is a willow short rotation coppice site in Risoe (DK-RCW) (55.68°N, 12.11°E) and the other one is a temperate deciduous beech forest site located in Soroe (DK-Sor) (55.48°N, 11.63°E). In Risoe site, the main willow species are *Salix schwerinii* × *S. viminalis* × *S. vim.* and *Salix triandra* × *S. viminalis*. Rapeseed (*Brassica napus*) was grown in the nearby field. The eddy covariance system has been operated from 2012 until now. Regular UAS flight campaigns were conducted at Risoe during the growing seasons of 2016 and 2017. In the Soroe site, the dominant tree species are European beech (*Fagus sylvatica* L.) and approximately 20% conifers, Norway spruce (*Picea abies* (L.) Karst.) and European larch (*Larix decidua* (Mill.)). The Soroe flux site has been operated since 1996 and has 22-year long-term eddy covariance observations until now. Details of this site are reported in Pilegaard et al. (2011) and Wu et al. (2012).

Figure 3-1. The location of the eddy covariance sites. Risoe is planted with willow bioenergy plantation. Soroe is a site with temperate deciduous beech forest.

The in-situ measurements used in this study include the standard eddy covariance and meteorological observations (e.g. latent heat flux, sensible heat flux, GPP, incoming shortwave radiation, outgoing shortwave radiation, incoming longwave radiation, outgoing longwave radiation, air temperature, vapor pressure deficit, wind speed, wind direction and air pressure), PAR sensor observations (above and below the canopy), LAI measurements from Licor LAI2200c and in-situ soil moisture meausurements.

4 Materials and methods

The designed UAS monitoring system including the imaging payload and models for simulation of land surface fluxes is shown in Figure 4-1. This system is flexible for various UAS platforms (rotary, fix wing or hybrid types). The only requirement of the platform is that it can take 2 kg payload. This system can be applied under various weather conditions (sunny, cloudy and overcast). To test this monitoring system, pilot studies were conducted in a willow short rotation coppice site Risoe, where eddy covariance systems can provide data to validate this monitoring system.

An UAS imaging payload consisting of a six band multispectral camera, a thermal infrared camera and a normal RGB camera was deployed on a hexacopter to conduct flight campaigns at eddy covariance sites. With radiometric and geometric correction and noise reduction, the UAS imagery was processed into high-quality UAS orthophotos. These UAS based multispectral, thermal and surface elevation data was further used as inputs of the ‘top-down’ snapshot models to estimate soil moisture, net radiation (Rn), ET and GPP. Further, to temporally interpolate the snapshot estimates, the UAS data were used as inputs of the ‘SVEN’ model to continuously estimate GPP and ET. These simulated land surface fluxes were validated by the eddy covariance observations with a footprint model (Kljun et al., 2015). The integration of the UAS based VHR imagery with the ‘top-down’ models provides insights into explore the spatial and temporal scaling issues in remote sensing. For instance, the optimal spatial resolution to capture land surface fluxes and the methodologies to temporal upscaling the remote sensing based instantaneous simulation into diurnal and longer time scale estimates.

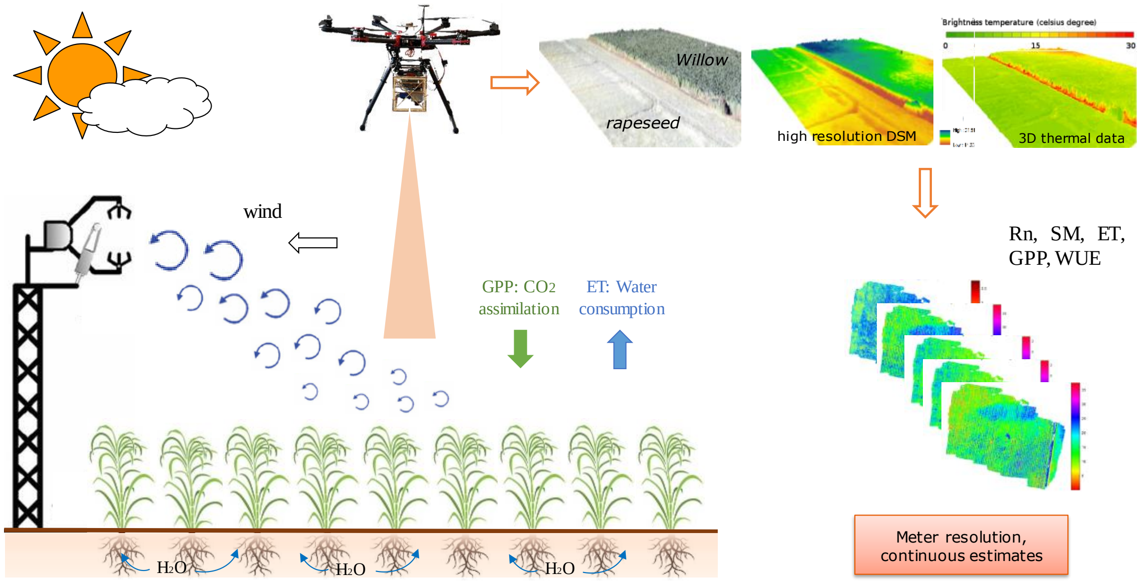

Figure 4-1. Designed UAS based monitoring system in this study. The UAS equipped with the imaging payload was used monitor the land surface conditions in a willow bioenergy plantation. The collected optical and thermal data were used as model inputs to simulate the net radiation (Rn), soil moisture (SM), evapotranspiration (ET), gross primary productivity (GPP) and water use efficiency (WUE) with high spatial resolution and continuous records. The simulated land surface fluxes were validated by the eddy covariance observations.

4.1 Unmanned aerial system

4.1.1 Platform

In this study, the flight campaigns were mainly conducted with a rotary wing platform, DJI hexacopter Spreading Wings S900 equipped with A2 flight controller (DJI, Shenzhen, China), as shown in Figure 4-2. The rotary wing platform has advantage of flexible taking off and landing, high manoeuvrability and hovering capability.

Figure 4-2. UAS platform (DJI S900) used in this study

4.1.2 Payload

The payload includes three parts, an imaging system, a navigation system and a micro-processor as shown in Figure 4-3. The imaging part includes three sensors, (i) a RGB camera, (ii) a thermal infrared camera and (iii) a multispectral camera. The RGB camera is a Sony DSC-RX100 to retrieve high accuracy digital surface elevation model. The thermal infrared camera FLIR tau2 324 (Wilsonville, OR, USA) is deployed to obtain the information of the land surface temperature. A six-band multispectral camera Tetra mini-MCA (Multispectral Camera Array, Tetracam, Chatsworth, CA, USA) was used to collect surface reflectance and calculate vegetation indices to infer the growth status of vegetation. These six bands include blue, light green, dark green, red, red edge and near infrared with the central wavelength of 470, 530, 570, 670, 710 and 800 nm, respectively. The full wavelength at half maximum is 10 nm. Details on the multispectral and thermal sensors can be found in Wang et al. (**I** and **III**).

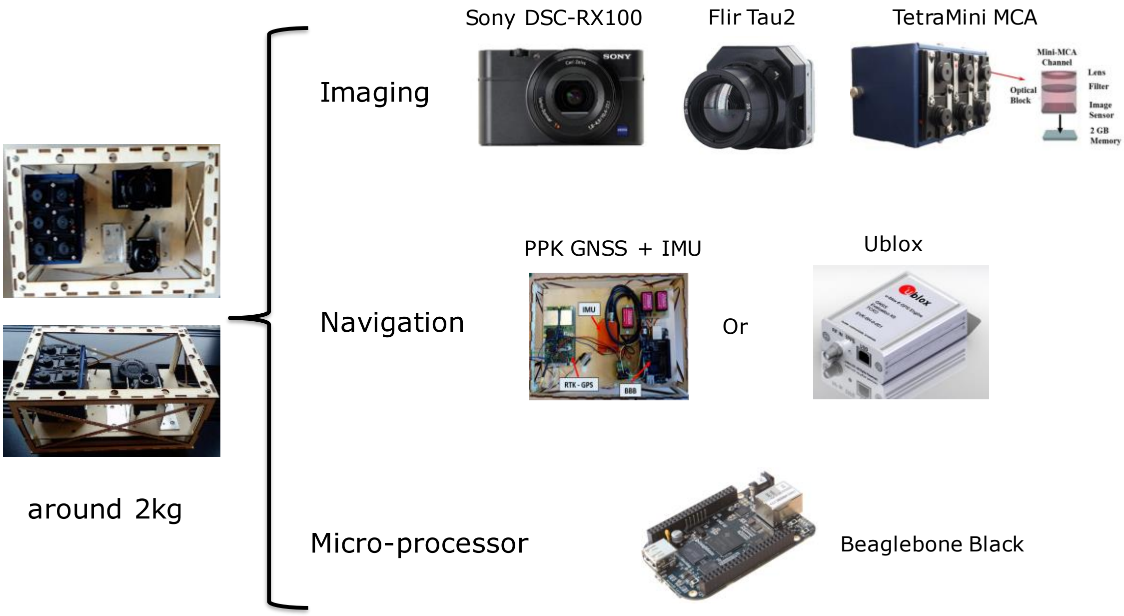

Figure 4-3. Components of the imaging payload designed in this study. The imaging part includes three sensor, a RGB camera, a thermal infrared camera and a multispectral camera. The navigation part can use either the post-processed kinematic (PPK) GNSS solution or single receiver GNSS solution of Ublox. The micro-processor is the Beaglebone Black.

4.2 Flight campaigns

UAS flight campaigns in the Risoe flux site were conducted in the growing seasons of 2016 and 2017 as shown in Table 4-1. These days include sunny and cloudy weather conditions. Detailed information on the weather conditions during the flight campaigns can be found in Wang et al. (**III** and **IV**). Figure 4-4 shows the typical paths of UAS flight campaigns at Risoe.

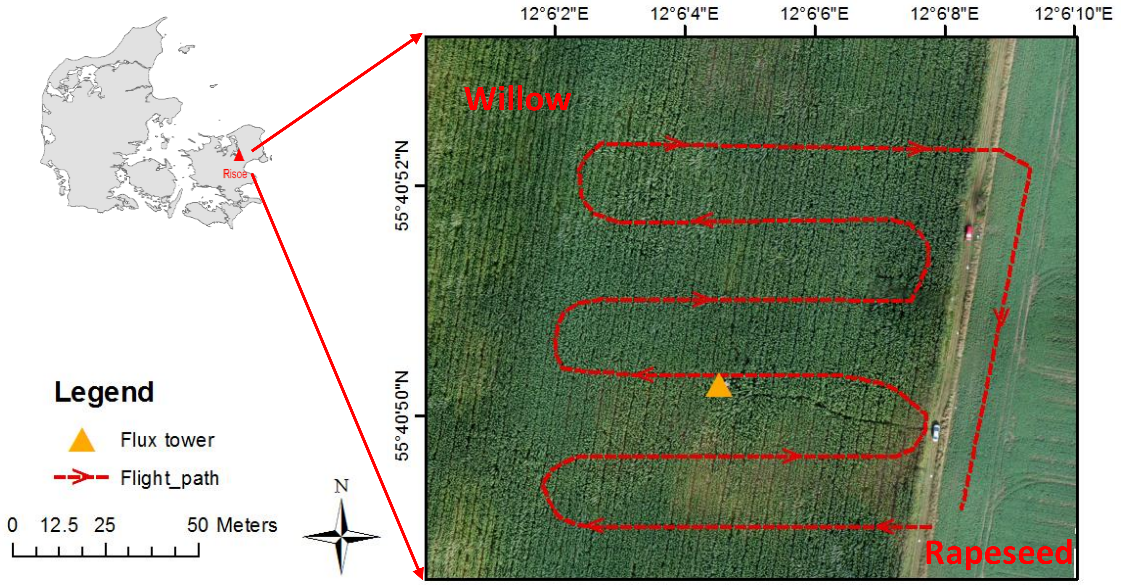

Figure 4-4. The typical flight paths of UAS campaigns conducted in Risoe

Table 4-1. Information on flight campaigns conducted at the Risoe site

Number	Date	Acquisition time	Weather condition
1	11-04-2016	11:13-11:26	Cloudy
2	02-05-2016	14:40-14:55	Cloudy
3	12-05-2016	10:44-11:55	Sunny
4	25-05-2016	10:11-10:23	Sunny
5	01-08-2016	10:06-10:14	Overcast
6	07-10-2016	11:41-11:55	Sunny
7	19-05-2017	12:07-12:19	Sunny
8	22-05-2017	10:15-10:28	Cloudy
9	26-05-2017	11:13-11:26	Sunny
10	18-06-2017	12:39-12:51	Cloudy

4.3 Sensor calibration and image processing

A high quality of the remotely sensed data from UAS is essential for performing quantitative land surface modelling. The high latitude regions e.g. Denmark have a high frequency of the cloudy and overcast weather (Wang et al., 2018a). UAS flight campaigns sometimes have to be conducted under suboptimal weather conditions. In order to produce UAS imagery with high quality and accuracy, several strategies were proposed in this thesis. First, a precisely geometric and radiometric calibration was conducted in the laboratory. The laboratory experiments include geometric calibration to retrieve lens distortion parameters based on the Brown-Conrady distortion model, noise correction, vignetting correction and radiometric calibration to link the image digital number to the intensities of spectral radiance. Particularly, the light intensities of the calibration facility were designed to match with the typical outdoor conditions in high latitudes and the calibration was conducted with low illumination conditions. Further, outdoor experiments were conducted with homogeneous targets to compare the sensitivity of different multispectral channels. Finally, the flight campaigns with MCA were conducted under both sunny and cloudy conditions. UAS orthophotos were generated from hundreds of small footprint images acquired from the UAS by using the Agisoft Photoscan software, which is based on the Structure-from-Motion (Westoby et al., 2012).

A multivariate statistical method, the Tucker tensor decomposition (Mørup, 2011), was tested to remove the cloud shadows in the multispectral images collected under variable irradiance conditions due to overlapping of images. The UAS multispectral imagery can be understood as data cubes (four-way tensors), consisting of two spatial modes, denoted as x and y, and one spectral and one temporal dimension. As shown in Eq. 4-1, the four-way tensor can be decomposed into a core, four modes (two in the spatial domains, one in the spectral domain and one in the time domain) and a residual. By choosing different percentages of signals in decomposed modes, the reconstructed image can have different levels of signals from the raw image. As the cloud shadow changed with time, the cloud shadow in the UAS imagery can be removed by reducing the signals in the time domain for image reconstruction. Finally, the accuracy of reflectance from the produced orthophotos were examined. For details on this methodology, please refer to Wang et al. (**I**).

$$X_{i_1 i_2 i_3 i_4} = \sum_{j_1=1}^{J_1} \sum_{j_2=1}^{J_2} \sum_{j_3=1}^{J_3} \sum_{j_4=1}^{J_4} g_{j_1 j_2 j_3 j_4} a_{i_1 j_1} b_{i_2 j_2} c_{i_3 j_3} d_{i_4 j_4} + e \quad \text{(Eq. 4-1)}$$

Where i_1, i_2, i_3, i_4 represent the spatial, spectral and temporal dimensions of the four-way tensor obtained from UAS imagery, respectively. j_1, j_2, j_3, j_4 represent the four dimensions of the tensor core. a, b, c and d are four modes. e is the residual and ideally should be noise.

4.4 Land surface modelling framework

A joint 'top-down' ET and GPP model constrained by the same environmental variables was proposed in this study by expanding the capabilities on the PT-JPL ET model (Fisher et al., 2008) and merging it with the LUE GPP model

(Potter et al., 1993) as shown in the Figure 4-5. This joint ET and GPP model calculates the potential rates of ET and GPP, and then estimates the actual values based on the environmental constraints. The vegetation stressors, e.g. the air temperature constraint, the fraction of green vegetation and plant moisture constraint, could be obtained from meteorological observations or the remotely sensed data. Further, this joint model incorporated a cloudiness index (CI) representing the fraction of diffuse PAR to improve the estimation of the surface fluxes in Wang et al. (**II**). Based on the model, a global sensitivity analysis Sobol' (Sobol, 2001) was used to quantify the first order and global sensitivity of model inputs to the inputs of various environmental factors. Along with a statistical regression analysis, path analysis (Bassow & Bazzaz, 1998; Huxman et al., 2003), the influence of the environmental factor (the diffuse radiation fraction) on the GPP, ET, incident light use efficiency, evaporative fraction and water use efficiency (WUE) was quantified at the Soroe site.

One of the most relevant parameters to constrain ET from the potential to the actual values is soil moisture. The soil moisture constraint for this joint model can be calculated from either in-situ observations as Wang et al. (II) or the temperature-vegetation triangle approach as Wang et al. (III) depending on the research objective. The temperature-vegetation triangle approach is based on the theory that soil moisture influences the ET rate and surface temperature. It utilizes the remotely sensed optical and thermal data and has been widely applied to estimate the soil moisture and ET with satellite or manned airborne based data (Carlson et al., 1995; Garcia et al., 2014; Mallick et al., 2009; Moran et al., 1994; Sandholt et al., 2002; Stisen et al., 2007). However, in the previous studies, the linkage between the soil moisture estimates and surface fluxes is not always explicit. Thus, in the Wang et al. (II), the triangle approach was modified by considering the influence of the 3D canopy structure (height) to the surface fluxes, and applied this method with UAS optical and thermal observations to map spatial and temporal variability of soil moisture in the Risoe site. Finally, the soil moisture estimates from UAS were validated by the in-situ measurements at different depths and in space. The detailed workflow of this soil moisture study is shown in Figure 4-5.

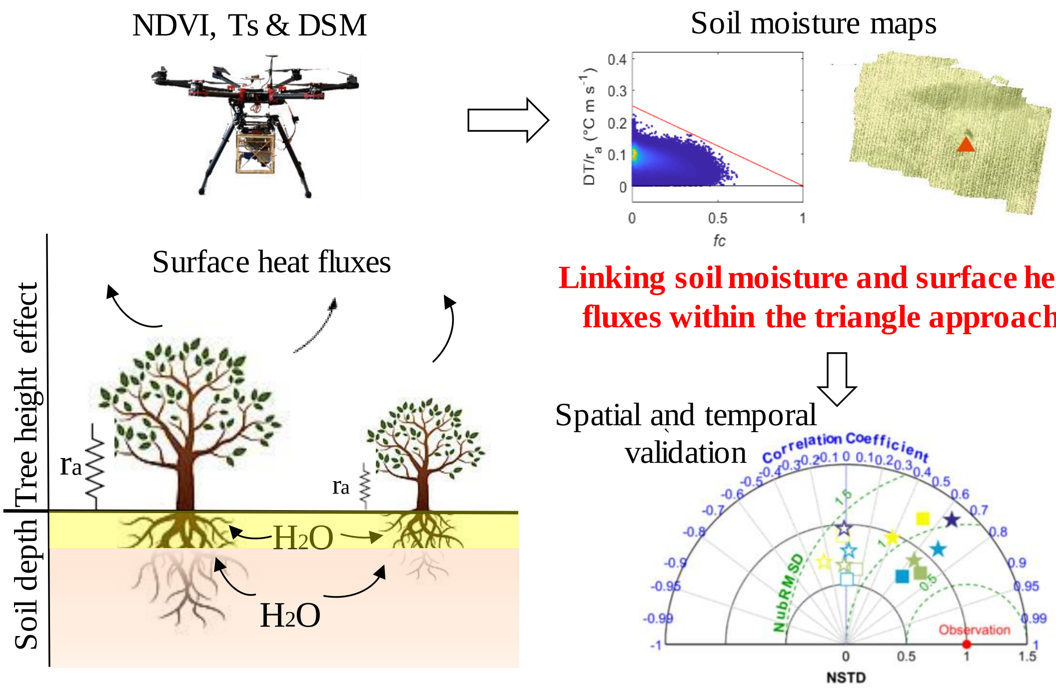

Figure 4-5. Workflow of soil moisture mapping from thermal and optical imagery. The NDVI, T_s and DSM information were collected by UAS in the field. By using the modified temperature-vegetation triangle approach, the spatial and temporal variabilities of soil moisture were estimated. Finally, the estimated soil moisture were compared with the spatial soil moisture measurements (2 campaigns) and temporally continuous soil moisture measurements at different depths (8 dates). For details on the Taylor diagram validation, refer to Figure 13 in Wang et al. (**III**).

Based on the joint model in Wang et al. (**II**) and the modified temperature-vegetation triangle approach in Wang et al. (**III**), Wang et al. (**IV**) utilized the optical and thermal data to estimate net radiation, ET, GPP and water use efficiency from high spatial resolution UAS imagery. The eddy covariance observations along with the footprint model was used to validate the simulated land surface fluxes from UAS imagery. Further, with the high spatial resolution maps of land surface fluxes, the importance of considering the heterogeneity of vegetation and eddy covariance source contribution to the model benchmark were evaluated by the semivariogram and an experiment to aggregate model inputs to different spatial resolution. In this way, the optimal spatial resolution to capture the land surface fluxes was also identified. The control factor on the spatial variability of the land surface fluxes was quantified. Finally, the importance of considering the changes in footprint in the diurnal upscaling from the instantaneous ET estimates to the diurnal values was tested.

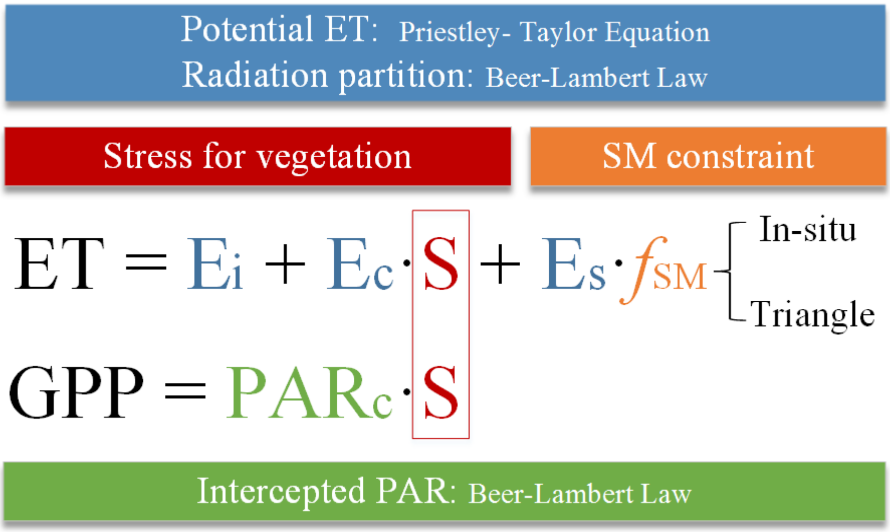

Figure 4-6. Schematic diagram representing the joint PT-JPL ET and LUE GPP model. ‘Ei’ is the evaporation from the intercepted water. ‘Ec’ is the potential transpiration. ‘S’ stands for the vegetation stressors. ‘Es’ is the potential evaporation from soil. The soil moisture constraint ‘f_{SM}’ can be obtained from either in-situ observations or the temperature-vegetation triangle approach.

Based on the snapshot model, the ‘top-down’ model was further developed to obtain a temporally dynamic model as shown in Wang et al. (**V**). This was achieved by including a module to predict the ground heat flux based on the force-restore’ method (Noilhan and Planton, 1989), and simple bucket models to simulate the dynamics of canopy wetness and soil water. Figure 4-7 shows the linkages between the snapshot model and the continuous model namely Soil-Vegetation, Energy, water and CO_2 traNsfer model (SVEN). This parsimonious continuous model requires limited data inputs and parameterization. It can be applied to temporally interpolate the simulated land surface conditions between the remote sensing data acquisitions.

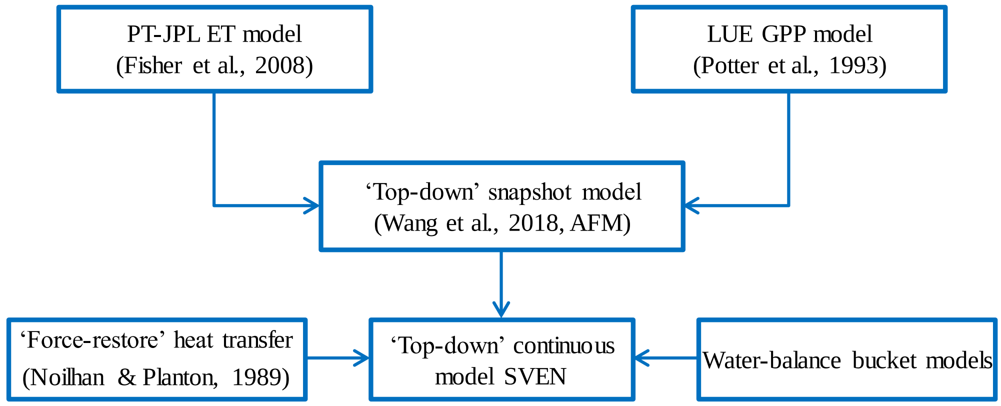

Figure 4-7. The development of the Soil-Vegetation, Energy, water and CO_2 traNsfer model (SVEN). The PT-JPL ET model (Fisher et al., 2008) and the LUE GPP model (Potter et al., 1993) were combined to the 'top-down' snapshot model (Wang et al., 2018) with the same environmental constraints. Further, the snapshot model was combined with the 'force-restore' heat transfer model and water balance bucket models to continuously estimate land surface fluxes.

Integrating in-situ observations or Earth Observations into models can provide better model parameterization and improve model simulations. One way is to perform model calibration. In Wang et al. (**II** and **V**), the Monte Carlo optimization method was used to calibrate the model parameters for the joint snapshot and continuous ET and GPP models using eddy covariance observations. The Monte Carlo method can efficiently generate the large data set of possible combined parameter values with given certain ranges of parameter values. By comparing the simulated ET and GPP with observations from the eddy covariance tower, the model can provide better simulation outputs of land surface fluxes. Furthermore, as the land surface model, which outputs multiple variables such as soil moisture, ET and GPP, can hardly simulate all variables equally well simultaneously (Sorooshian et al., 1993; Vrugt et al., 2003). Wang et al. (**V**) addressed this multiple objective optimization issue by using the Pareto front as Yapo et al. (1998). With the Pareto font analysis, the performance of the simulated surface temperature and soil moisture by the SVEN model was evaluated simultaneously. The optimum values from the Pareto front were identified to provide good estimates of both surface temperature and soil moisture, as they are the two key variables that determine fast changes in land surface fluxes. The calibration of SVEN in Wang et al. (V) with the snapshot simulation outputs from Wang et al. (IV) rather than from in situ eddy covariance observations, which makes the model applicable in areas without in-situ data.

Besides model calibration, model-based analysis and observation-based analysis were integrated with the purpose to understand better controls on GPP and ET and the role of diffuse/direct radiation. In Wang et al. (II), the path analysis, which is a multiple regression technique and considers the covariance among different variables (Bassow and Bazzaz, 1998; Li, 1975), was used to separate the direct and indirect effects from diffuse radiation to land surface fluxes and to assess sensitivity of GPP, ET and WUE to diffuse radiation. Additionally, based on the model based global sensitivity analysis, the first order and second order sensitivities from the model parameters to the simulated outputs were identified. The comparison between observation based analysis and model based analysis can assess if the ‘top-down’ model had similar sensitivity to diffuse light as the results from data mining methods. Additionally, this can provide a robust assessment of the direct and indirect effects from diffuse radiation to land surface fluxes.

5 Results

5.1 Sensor calibration and image processing

Results on the pixel wise sensor calibration of MCA with the low illumination conditions (spectral radiance from 0.01 to 0.2 $W \cdot m^{-2} \cdot sr^{-1} \cdot nm^{-1}$) are shown in Figure 5 of Wang et al. (**I**). With high coefficient of determination (R^2) and small root mean square deviations (RMSD), this laboratory calibration extended the sensor exposure time setting from 1 to 4 ms, which is suitable for the Mediterranean high irradiance conditions (Berni et al., 2009), to 1 to 8 ms, which is designed for the low irradiance high latitude condition. Using the high exposure time settings under low irradiance conditions can increase the image signal to noise ratios (SNRs). Further, with analysing the sensitivity of different MCA channels to the radiance (Figure 6 of Wang et al., **I**) and the outdoor experiments (Figure 7 of Wang et al., **I**), it is found that different channels have different sensitivities and the individual exposure settings for independent channels instead of the uniform setting can increase the image SNRs.

To remove the cloud shadow in the multispectral imagery, this study succeeded by using the Tensor decomposition as an example shown in Figure 5-1. The comparison between the corrected and un-corrected images shows a significant improvement for reflectance in the cloud shadow areas, as the red circle areas in Figure 5-1. With the proposed methodology in Wang et al. (I), our study demonstrated that it is possible to provide reliable reflectance with RSMD around 3% under low (solar radiance around 0.1 $W \cdot m^{-2} \cdot sr^{-1} \cdot nm^{-1}$) and variable irradiance conditions at 55° latitude. This quality of reflectance data is comparable to other studies in higher illumination regions (Berni et al., 2009; Laliberte et al., 2011).

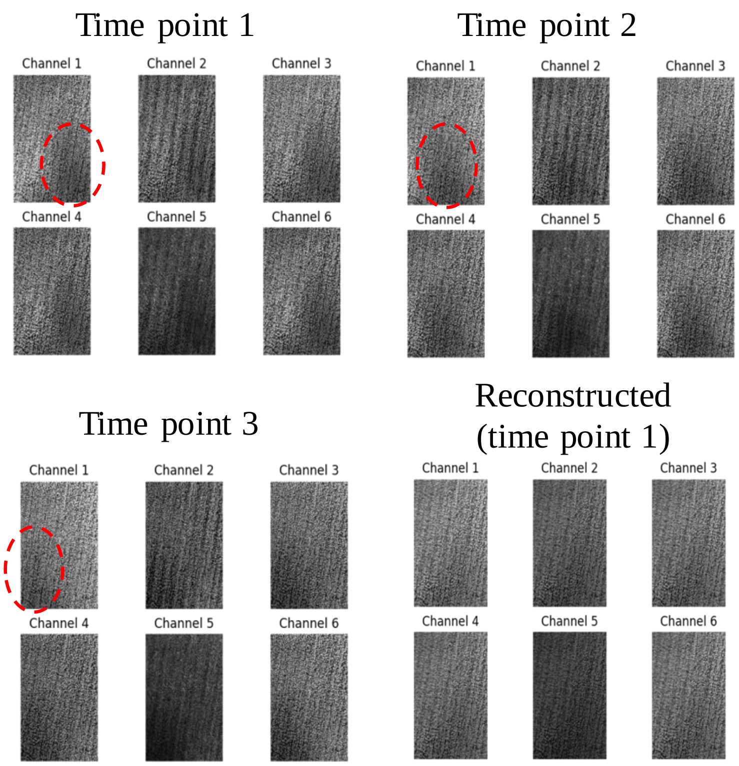

Figure 5-1. Cloud shadow removal by the tensor decomposition. The images are reflectance collected from the UAS campaigns in the willow plantation at three moments. The cloud shadow for each pair of images was highlighted with the red circles. It can be seen from cloud shadow has been removed in the reconstructed images.

With the thoroughly geometric and radiometric calibration of sensors and improved image processing procedures, UAS multispectral mapping can generate reliable and repeatable reflectance in low and variable irradiance conditions. Figure 5-2 shows an example of the produced orthophotos of surface temperature (T_S), NDVI and true colour images from the UAS thermal and multispectral images collected on 25th May 2016.

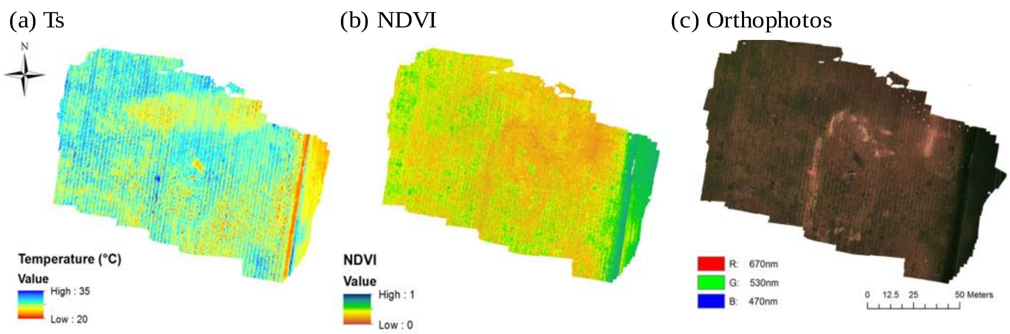

Figure 5-2. (a) UAS based surface temperature orthophotos, (b) Normalized Difference Vegetation Index (NDVI) and (c) True colour multispectral orthophoto on 25th May 2016.

5.2 Spatial variability of land surface fluxes

As a first step towards UAS based land surface modelling, the soil moisture was estimated from optical and thermal imagery in Wang et al. (**III**) by using the explicit linkage between the soil moisture and non-evaporative fraction within the temperature-vegetation triangle approach. Figure 11 of Wang et al. (**III**) shows the spatial validation of the estimated soil moisture. By aggregating the soil moisture estimates to different sizes of buffer zones (see example of buffer zones in Figure 1 of Wang et al. (**III**)), it is found that the best match between the estimates and the in-situ measurements is at 1.5 m, which corresponds to the observed average size of tree crown. Wang et al. (**III)** highlight the importance to consider the 3D canopy structure to the soil moisture and thermal data interpretation.

Furthermore, by comparing soil moisture observations at different soil depths as the results shown in Figure 13 of Wang et al. (**III**), it is found that the estimated soil moisture had highest correlation with soil moisture at the depth of 30-60 cm. This depth tends to be to the soil layer of higher root density for the willow plantation (Persson, 1995; Phillips et al., 2014). This agrees with the theory that the temperature-vegetation triangle approach detecting the soil moisture conditions through the transpiration rate (Carlson et al., 1995; Garcia et al., 2014; Mallick et al., 2009; Moran et al., 1994; Sandholt et al., 2002; Stisen et al., 2007). This shows the advantage of the temperature-vegetation triangle approach to reflect the root-zone soil moisture, which has significance to predict near-future vegetation anomalies (Qiu et al., 2014), over the thermal inertia or microwave based method, which only detect the soil moisture at the surface layer (< 10 cm) (García et al., 2013; Njoku et al., 2003).

In general, the modified temperature-vegetation triangle approach estimated the volumetric soil moisture with an accuracy of the correlation coefficient around 0.58-0.69 and RMSDs around 0.025 $m^3 \cdot m^{-3}$ in the Risoe site. Compared to other UAS based soil moisture studies (Hassan-Esfahani et al., 2015, 2017; Wang et al., 2018c) and manned airborne based studies (Fan et al., 2015; Sobrino et al., 2012), this study achieved a similar accuracy, but it requires limited ground measurements and independent of the model calibration. It has potential to be used for routinely application in the agricultural sites.

With the developed ‘top-down’ ET and GPP model (Wang et al., **II**) and the estimated soil moisture from the temperature-vegetation triangle approach to constrain the ET, the high spatial resolution net radiation, the fraction of the intercepted PAR, ET, GPP, evaporative fraction, light use efficiency and water use efficiency were estimated in Wang et al. (**IV**). By using the eddy covariance observations and the footprint model (Kljun et al., 2015), results indicate that our approach can simulate the instantaneous net radiation, ET, GPP and water use efficiency with RMSDs of 31.6 $W \cdot m^{-2}$, 41.2 $W \cdot m^{-2}$, 3.12 $\mu mol \cdot C \cdot m^{-2} \cdot s^{-1}$ and 0.35 $g \cdot C \cdot kg^{-1}$, respectively. More validation results on other variables are shown in Figure 7 of Wang et al. (**IV**). The accuracy of the simulated ET is similar or slightly better to other studies (Brenner et al., 2017; Hoffmann et al., 2016; Ortega-Farías et al., 2016). This may be due to the fact that this joint model is based on the PT-JPL ET model (Fisher et al., 2008), which is a vegetation driven approach and relies less on the accuracy of the thermal and soil moisture data (McCabe et al., 2017). Additionally, this site is a radiation controlled ecosystem (Wang et al., 2018a) and our methodology has a good estimation of Rn as shown in Figure 7 (c) of Wang et al. (**IV**).

To verify the simulated high spatial resolution patterns of fluxes, the VHR model inputs (as NDVI and T_b in Figure 5-2) were aggregated to different spatial resolution to simulated land surface fluxes. It was found there is a degradation trend with coarser spatial resolution as shown in Figure 13 of Wang et al. (**IV**). This also confirms the accuracy of our simulated ET and GPP patterns. Otherwise, if the simulated pattern were wrong, there would not be such a degradation. Additionally, variations of the eddy covariance footprint during the course of the day can sample different areas around the tower, as an example of Figure 5-3. As shown in Figure 10 of Wang et al. (**IV**), the good results in the diurnal simulation provides confidence in our simulated spatial patterns to some extent.

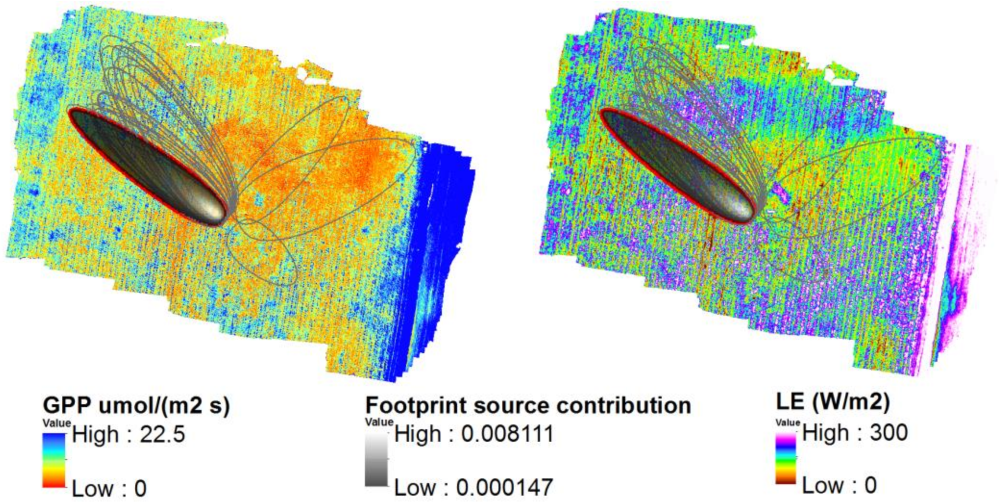

Figure 5-3. An example of the simulated GPP and LE on 25th May 2016. The circles indicates the variations of the eddy covariance footprint. The shaded area is the footprint location when the UAS flight campaign was conducted. The value in the shaded area indicates the source contribution of the footprint.

Semivariogram analysis was used to explore the control factor dominating the spatial variability of the land surface fluxes, Figure 12 of Wang et al. (**IV**). It was found that during the early growth stage, the spatial pattern has highest spatial correlation at 1.5-2 m. Further, the model simulation performance with different aggregated spatial resolutions shows that there is a change of model performance at 1.5 m, as shown in Figure 13 of Wang et al. **IV**. Together with the spatial validation results of soil moisture in Figure 11 of Wang et al. (**III**), these findings indicate the tree crown size may determine the spatial variability of the land surface fluxes. The consistent simulation performance with the spatial resolution from 0.03 to 1.5 m in Figure 13 of Wang et al. **IV** also implies that the spatial resolution at the tree crown size may be enough for benchmarking models with the eddy covariance observations. This semivariogram based spatial analysis of VHR imagery can also help to determine optimum flight height and spatial resolution to estimate ET and GPP for subsequent flights.

5.3 Temporal dynamics of land surface fluxes

As a first step to temporally upscale the instantaneous estimates of ET and GPP from remotely sensed data to the longer time scales (Gentine et al., 2007; Morillas et al., 2014), Wang et al. (**IV**) addressed the upscaling process from instantaneous to diurnal. As shown in Figure 5-3, the VHR imagery provides opportunities to account for the change of the eddy covariance footprint. Results of Figure 10 (c) in Wang et al. (**IV**) show that the temporal upscaling approach considering the change of the footprint performs better than the classic approach assuming the constant evaporative fraction, which is widely used in other studies (Brutsaert and Sugita, 1992; P. D. Colaizzi et al., 2006). This implies that the high-resolution UAS imagery can be a useful tool to benchmark the model with the eddy covariance observations in the temporal upscaling process from the instantaneous to the diurnal.

To interpolate estimates of land surface fluxes between different days without UAS data acquisitions, the Soil-Vegetation, Energy, water and CO_2 traNsfer model (SVEN) was developed to simulate land surface fluxes for days without UAS acquisitions during the growing seasons of 2016. Based on the instantaneous estimates from the snapshot models (Wang et al., **IV**), the SVEN model achieved satisfactory simulation results with RMSDs of simulated daily land surface temperature, soil moisture, GPP and ET equal to 2.17°C, 2.68% $m^3 \cdot m^{-3}$, 3.01 $g \cdot C \cdot m^{-2} \cdot d^{-1}$ and 16.88 $W \cdot m^{-2}$, respectively. This study demonstrates the potential of UAS multispectral and thermal mapping to continuously monitor land surface fluxes.

Additionally, with the 11-year long-term eddy covariance observations, Wang et al., (**II)** identified the influence of main environmental factors on the land surface fluxes at the temperate deciduous forest at Soroe site at different months as shown in Figure 5-4. It can be seen that this ecosystem is radiation controlled, as both GPP and ET are highly determined by the radiation changes. CI represents the contribution of the diffuse radiation fraction. It was found using path analysis that CI contributes approximately 11% variations of GPP, 3% variations of ET and 8% variations of transpiration during the growing season from May to October.

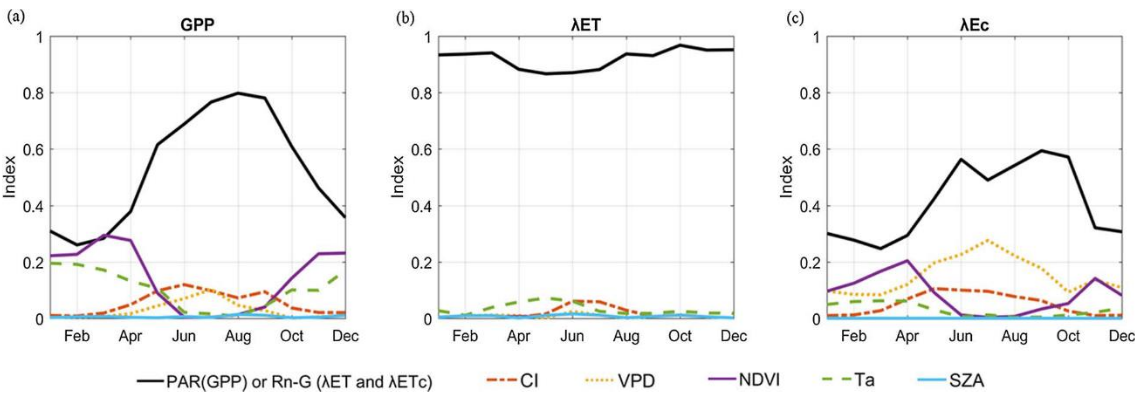

Figure 5-4. The first order sensitivity of the environmental factors to the variables of the (a) GPP, (b) λET (the total latent heat flux), and (c) λETc (the latent heat flux for the transpiration part). CI represents the diffuse radiation effects. VPD is the vapour pressure deficit. NDVI represents the vegetation growths and Ta is the air temperature and SZA is the sun zenith angle. (Wang et al., **II**)

Through the statistical based path analysis and the model based global sensitivity analysis, the independent and joint effects of the diffuse radiation fraction on GPP, ET, incident light use efficiency, evaporative fraction and water use efficiency were quantified. Results showed that the influence of the diffuse radiation fraction on GPP is larger than that on ET and this leads to an increase of WUE. Due to the interaction of diffuse PAR with plant canopies, the largest model improvements using the diffuse radiation fraction for GPP and ET occurred during the growing season and for the transpiration component, as suggested by comparisons to sap flow measurements. Regarding the influence of diffuse radiation to GPP and transpiration, the diffuse radiation fraction was incorporated into the GPP and transpiration simulation as an environment constraint. Additionally, it was found that due to the increased longwave emission from clouds, surface temperature gets higher and closer to optimum, boosting GPP and transpiration in the temperature-limited high latitude ecosystem, which could be consider for future model improvements.

6 Conclusions

This thesis designed an operational UAS based monitoring system to continuously monitor land surface fluxes at very high spatial resolution under various weather conditions. This study was demonstrated in a willow bioenergy short rotation coppice (DK-RCW) and a deciduous beech forest (DK-Sor). 'Top-down' ET and GPP models were developed and combined with the optical and thermal UAS imagery to simulate the land surface fluxes. This thesis led us to the following conclusions to answer our research objectives:

(i) By thoroughly calibration of UAS sensor and improved image processing procedures for the low and variable irradiance conditions at norther latitudes, this thesis achieved an accuracy to obtain high quality of reflectance imagery with root mean square deviations (RMSDs) around 3%. This shows the potential of UAS mapping for quantitative remote sensing research under challenging irradiance conditions such as those encountered in Denmark.

(ii) With a 'top-down' ET and GPP model and the modified temperature-vegetation triangle approach, satisfactory accuracy of the simulated net radiation, the root-zone soil moisture, ET, evaporative fraction, GPP, light use efficiency and water use efficiency were obtained in DK-RCW. By using high spatial resolution maps of the simulated land surface fluxes from UAS imagery, it was found that the tree crown size (around 1.5 for the dense vegetation condition in our site) controls the spatial variability of the land surface fluxes and simulation with the spatial resolution at the tree crown size is sufficient to capture the spatial variability of fluxes, which will allow higher flying heights and higher coverage of UAS imagery.

(iii) In the temporal upscaling of the land surface fluxes (ET and GPP) from the instantaneous to the diurnal, it was found that it is important to consider the change of the eddy covariance footprint during the course of the day, when benchmarking the model with the eddy covariance observations while assuming a constant evaporative fraction during the day lead to degradation in the accuracy of ET estimates. To achieve continuous modeling of land surface fluxes (e.g. filling temporal gaps between UAS flights), the system merged a 'top-down' remote sensing model for GPP and ET with time-dynamic modules for ground heat flux and water infiltration. This model for temporal interpolation can also be potentially applied with other remote sensing data e.g. satellites. Furthermore, with 11-year long term eddy covariance observations, the independent and joint effects from diffuse radiation to the temporal variability of GPP and ET were identified. At this ecosystem, diffuse radiation plays a crucial role to enhance ecosystem light use efficiency and water use efficiency. This effect was incorporated into the joint ET and GPP model to constrain transpiration and GPP to make is suitable to use from overcast conditions.

This UAS optical and thermal remote sensing based monitoring framework can provide spatially resolved near real time information on land surface fluxes. This information is valuable to optimize practical applications for agricultural and natural ecosystems. The unprecedentedly high spatial resolution can be used to examine scaling issues, identify spatial heterogeneity and benchmark models with eddy covariance fluxes. Further, this monitoring system has also ability to temporal upscaling the instantaneous estimates of land surface fluxes to the daily or longer time scales. Additionally, this system requires limited ground measurements and can be applied in the data scarce regions.

7 Future perspectives

7.1 Potential applications of this system

This UAS monitoring framework has the ability to provide VHR and continuous metrics on vegetation growth and vegetation water use: reflectance, vegetation indices, surface temperature, net radiation, ET, GPP and water use efficiency. These valuable spatial and temporal metrics are potentially beneficial for practical applications (food and bioenergy production) and fundamental science (remote sensing, ecohydrological research, micrometeorology).

For the agricultural production, there is an urgent need to increase the sustainability of our food systems. One way is to provide more comprehensive metrics beyond crop yields per hectare (Sukhdev, 2018), capable to assess ecosystem services related with crop water use, carbon fixation or cooling/warming effects from land (Wallace, 2000). These kind of metrics have the potential to inform policymakers, farmers and agribusinesses to avoid negative impacts on the managed systems. Currently, agriculture is undergoing a fourth revolution triggered by the exponentially increasing use of information technology and autonomous systems (Walter et al., 2017). For example, at the farm scale, precision agriculture is a management strategy to increase long-term, site-specific production efficiency and productivity while minimizing the risks of excessive chemical environmental pollution or yield loss due to insufficient inputs (Earl et al., 1996; Moran et al., 1997). Precision agriculture highly relies on the timely spatial information on crop and soil conditions (Moran et al., 1997). Our UAS monitoring framework is able to provide VHR maps of metrics such as soil moisture, ET, GPP and water use efficiency, which are indicators to describe the actual crop physiology and physical state. On long-term applications, i.e. if crop and site specific data are available and related to crop specific harms, the obtained variables can be interpreted as early risk indicators for local crop damage or reduced productivity. The high spatial resolution makes it possible to identify patches with earliest responses to environmental stresses or infections, which could be used as an early warning system to take proactive action for crop management and avoid large-scale damage.

For remote sensing, UAS makes it possible to examine surface processes at unprecedented scale, i.e. 2-3 orders of magnitude higher than satellite systems, in both sunny and cloudy conditions. The UAS provided VHR multispectral, hyperspectral and thermal data for land surface flux simulation are thus complementary to other remote sensing techniques (e.g. satellite or manned airborne). With the rapid development of satellite remote sensing techniques, satellite missions (e.g. the Planet CubeSat constellation) can provide high temporal frequency broadband spectral data (i.e. blue, green, red and NIR) with 1-10m spatial resolutions (McCabe et al., 2017), given cloud-free conditions. With the VHR optical UAS data, it can easily be tested, whether the resolution of satellite imagery is sufficient for monitoring the heterogeneity of water and carbon use by crops, which depends on the site, season, climate and management as shown in our spatial analysis. In our homogeneous eddy covariance site of this study, VHR UAS data still provide considerable advantages to monitor water and carbon use for the patchy early growth stage of vegetation when the canopy cover is not complete. As demonstrated by other studies, this type of UAS monitoring system is an important tool for quantification of carbon and water fluxes in farming systems with higher structural spatial variability, e.g. agroforestry systems (Kustas et al., 2018; Zarco-Tejada et al., 2012). Furthermore, VHR thermal and hyperspectral data, which are up to centimeter level, are still not available from satellites, even including near future developments.

In micrometeorology and ecohydrological research, eddy covariance observations are often used for benchmarking land surface or remote sensing models. VHR UAS data provide extended opportunities to benchmark models more precisely with eddy covariance observations. As demonstrated in our study, GPP and ET model validation within the eddy covariance footprint using the arithmetic mean of the footprint, is biased, especially when the sites are more heterogeneous than in the investigated willow plantation. For micrometeorology, VHR optical and thermal imagery has the potential to quantify issues from so far unmeasurable small-scale land surface heterogeneity, which compromise the representativeness of eddy covariance flux measurements. So far, the horizontal heterogeneity was mainly considered at larger spatial scales around flux towers, but horizontal heterogeneity within the footprint in a homogeneous looking site can now be investigated with UAS technology. UAS based VHR maps of energy exchange are a promising means to further observe the notorious lack of energy balance closure as found in the majority of micrometeorological studies (Metzger, 2018; Stoy et al., 2013; Xu et al., 2017). These maps can now be related to solve the discrepancy between land surface conditions measured at the eddy covariance tower and the effective states within the footprint (Vivoni, 2012).

7.2 Platform and sensor techniques

A hexacopter DJI S900 was mainly used in this study to deploy with the imaging payload for data collection. However, this UAS platform has limited payload capacity and flight duration time. To cover a large area, a fixed wing platform or a hybrid platform that combines rotatory and fixed wing's advantages could be flown for this research. The advantages of using a rotary wing vehicle rather than a fixed wing vehicle include the capability of vertically taking off and landing, and the ability to hover above a waypoint. In contrast, the merits of a fixed wing platform are the possibility to reach a larger survey coverage because of higher speed and longer flight time. However, the hybrid platform, which combines rotary wing and fixed wing techniques, has the advantages of both platforms. For example, one of these advanced hybrid platforms developed during the Smart UAV project by the Danish company Sky-Watch and the Technical University of Denmark (Bandini et al., 2018).

The growth of UAS and satellite constellation techniques (e.g. Planet Cubesat) promoted scientists and commercial business interest to look at systems that operate in between or are a hybrid of UAS and satellites. High Altitude Pseudo-Satellite (HAPS), e.g. Airbus Zephyr S and T, is a promising technique to fill a capability gap between satellites and UAS. Zephyr can navigates to hundreds or thousands of kilometres away with the beyond line of sight (BLOS) capabilities. HAPS are systems or platforms that usually float or operate for long periods at the stratosphere. The benefits of HAPS is that they can stay stationary, but are also manoeuvrable and potentially easier to deploy. They can provide a longer duration of flight relative to UAS.

The imaging systems of this study include RGB, multispectral and thermal infrared cameras. The next steps to make the system more operational should aim to estimate the land surface energy, water and CO_2 fluxes from data only from the UAS. For instance, a radiometer with a cosine receptor can be installed on the UAS to measure incoming shortwave radiation. Wind speed can be estimated using a UAS with a pitot tube (Cho et al., 2011).

Towards improving the accuracy of monitoring land surface fluxes, other remote sensing techniques (e.g. hyperspectral, LiDAR and microwave sensors), as shown in Figure 2-2, can be integrated into the UAS based monitoring system. Hyperspectral sensors are able to provide more spectral reflectance and indices and this can be used to improve flux estimation, for instance, UAS based photochemical reflectance index (PRI) or fluorescence (Zarco-Tejada et al., 2012, 2013). The SIF signals directly link to the vegetation photosynthesis rates and can be utilized to detect vegetation stress, GPP and transpiration estimation. LiDAR can be applied to generate dense cloud and estimate the canopy structure parameters, e.g. LAI, the canopy height and density. UAS based microwave sensors can be utilized to monitor soil moisture.

7.3 Modelling and model-data integration techniques

The ‘top-down’ models were applied in this study to estimate the surface-atmosphere flux exchanges. However, these models are originally developed for coarser resolution satellite based simulations. They neglect the horizontal interactions between neighbourhood pixels and are one-dimensional simulation approaches. Large eddy simulations (LES) or other computational fluid dynamics models can consider the horizontal interactions between each pixel. LES can be combined with VHR data obtained from UAS to understand the horizontal interactions for the surface-atmosphere flux exchanges.

Machine learning and data mining algorithms, e.g., artificial neural networks, support vector machine and deep learning, are an essential tool in the data-driven analysis in this big data era. Machine learning can be utilized to identify the key spectral signals related to the biophysical and biochemical parameters of vegetation to improve the early stress or disease detection for vegetation (Zarco-Tejada et al., 2018) or simulating the surface-atmosphere flux exchanges (Moreno-Martínez et al., 2018).

In this study, the Bayesian approach was used to calibrate the model parameters to integrate model and data. Besides the model parameter calibration, other model-data fusion techniques, e.g. data assimilation, can also be used to improve modelling performance. The data assimilation approaches, e.g. ensemble Kalman filter, three-dimensional or more advanced four-dimension variational differential assimilation techniques, can update the state variables, e.g. land surface temperature or soil moisture in the SVEN model, to improve the model simulation and prediction abilities.

8 References

Anderson, K. and Gaston, K. J.: Lightweight unmanned aerial vehicles will revolutionize spatial ecology, Front. Ecol. Environ., 11(3), 138–146, doi:10.1890/120150, 2013.

Anderson, M. C., Kustas, W. P., Norman, J. M., Hain, C. R., Mecikalski, J. R., Schultz, L., González-Dugo, M. P., Cammalleri, C., D'Urso, G., Pimstein, A. and Gao, F.: Mapping daily evapotranspiration at field to continental scales using geostationary and polar orbiting satellite imagery, Hydrol. Earth Syst. Sci., 15(1), 223–239, doi:10.5194/hess-15-223-2011, 2011.

Baldocchi, D. D.: Assessing the eddy covariance technique for evaluating carbon dioxide exchange rates of ecosystems: past, present and future, Glob. Chang. Biol., 9(4), 479–492, doi:10.1046/j.1365-2486.2003.00629.x, 2003.

Bandini, F., Lopez-Tamayo, A., Merediz-Alonso, G., Olesen, D., Jakobsen, J., Wang, S., Garcia, M. and Bauer-Gottwein, P.: Unmanned aerial vehicle observations of water surface elevation and bathymetry in the cenotes and lagoons of the Yucatan Peninsula, Mexico, Hydrogeol. J., 1–16, 2018.

Bassow, S. L. and Bazzaz, F. A.: How environmental conditions affect canopy leaf-level photosynthesis in four deciduous tree species, Ecology, doi:10.1890/0012-9658(1998)079[2660:HECACL]2.0.CO;2, 1998.

Berni, J., Zarco-Tejada, P. J., Suarez, L. and Fereres, E.: Thermal and Narrowband Multispectral Remote Sensing for Vegetation Monitoring From an Unmanned Aerial Vehicle, IEEE Trans. Geosci. Remote Sens., 47(3), 722–738, doi:10.1109/TGRS.2008.2010457, 2009.

Brenner, C., Thiem, C. E., Wizemann, H. D., Bernhardt, M. and Schulz, K.: Estimating spatially distributed turbulent heat fluxes from high-resolution thermal imagery acquired with a UAV system, Int. J. Remote Sens., 38(8–10), 3003–3026, doi:10.1080/01431161.2017.1280202, 2017.

Brutsaert, W. and Sugita, M.: Application of self-preservation in the diurnal evolution of the surface energy budget to determine daily evaporation, J. Geophys. Res., doi:10.1029/92JD00255, 1992.

Carlson, T. N., Gillies, R. R. and Schmugge, T. J.: An interpretation of methodologies for indirect measurement of soil water content, Agric. For. Meteorol., 77(3–4), 191–205, doi:10.1016/0168-1923(95)02261-U, 1995.

Cho, A., Kim, J., Lee, S. and Kee, C.: Wind estimation and airspeed calibration using a UAV with a single-antenna GPS receiver and pitot tube, IEEE Trans. Aerosp. Electron. Syst., 47(1), 109–117, doi:10.1109/TAES.2011.5705663, 2011.

Clevers, J. G. P. W. and Kooistra, L.: Using hyperspectral remote sensing data for retrieving canopy chlorophyll and nitrogen content, IEEE J. Sel. Top. Appl. Earth Obs. Remote Sens., 5(2), 574–583, doi:10.1109/JSTARS.2011.2176468, 2012.

Colomina, I. and Molina, P.: Unmanned aerial systems for photogrammetry and remote sensing: A review, ISPRS J. Photogramm. Remote Sens., 92, 79–97, doi:10.1016/j.isprsjprs.2014.02.013, 2014.

Damm, A., Paul-Limoges, E., Haghighi, E., Simmer, C., Morsdorf, F., Schneider, F. D., van der Tol, C., Migliavacca, M. and Rascher, U.: Remote sensing of plant-water relations: An overview and future perspectives, J. Plant Physiol., 227, 3–19, doi:10.1016/j.jplph.2018.04.012, 2018.

Earl, R., Wheler, P. N., Blackmore, B. S. and Godwin, R. J.: Precision farming-the management of variability, J. Inst. Agric. Eng., 51(4), 18–23 [online] Available from: http://agris.fao.org/agris-search/search.do?recordID=US201302863265, 1996.

Fan, L., Xiao, Q., Wen, J., Liu, Q., Tang, Y., You, D., Wang, H., Gong, Z. and Li, X.: Evaluation of the airborne CASI/TASI Ts-VI space method for estimating near-surface soil moisture, Remote Sens., 7(3), 3114–3137, 2015.

Farmer, D., Sivapalan, M. and Jothityangkoon, C.: Climate, soil, and vegetation controls upon the variability of water balance in temperate and semiarid landscapes: Downward approach to water balance analysis, Water Resour. Res., doi:10.1029/2001WR000328, 2003.

Fisher, J. B., Tu, K. P. and Baldocchi, D. D.: Global estimates of the land-atmosphere water flux based on monthly AVHRR and ISLSCP-II data, validated at 16 FLUXNET sites, Remote Sens. Environ., 112(3), 901–919, doi:10.1016/j.rse.2007.06.025, 2008.

Fisher, J. B., Melton, F., Middleton, E., Hain, C., Anderson, M., Allen, R., McCabe, M., Hook, S., Baldocchi, D., Townsend, P. A., Kilic, A., Tu, K., Miralles, D., Perret, J., Lagouarde, J.-P., Waliser, D., Purdy, A. J., French, A., Schimel, D., Famiglietti, J. S., Stephens, G. and Wood, E. F.: The Future of Evapotranspiration: Global requirements for ecosystem functioning, carbon and climate feedbacks, agricultural management, and water resources, Water Resour. Res., doi:10.1002/2016WR020175, 2017.

Gamon, J. A.: Optical sampling of the flux tower footprint, Biogeosciences Discuss., 12(6), 4973–5014, doi:10.5194/bgd-12-4973-2015, 2015.

Garbulsky, M. F., Peñuelas, J., Gamon, J., Inoue, Y. and Filella, I.: The photochemical reflectance index (PRI) and the remote sensing of leaf, canopy and ecosystem radiation use efficiencies. A review and meta-analysis, Remote Sens. Environ., doi:10.1016/j.rse.2010.08.023, 2011.

Garcia, M., Fernández, N., Villagarcía, L., Domingo, F., Puigdefábregas, J. and Sandholt, I.: Accuracy of the Temperature-Vegetation Dryness Index using MODIS under water-limited vs. energy-limited evapotranspiration conditions, Remote Sens. Environ., 149(October), 100–117, doi:10.1016/j.rse.2014.04.002, 2014.

García, M., Sandholt, I., Ceccato, P., Ridler, M., Mougin, E., Kergoat, L., Morillas, L., Timouk, F., Fensholt, R. and Domingo, F.: Actual evapotranspiration in drylands derived from in-situ and satellite data: Assessing biophysical constraints, Remote Sens. Environ., 131, 103–118, doi:10.1016/j.rse.2012.12.016, 2013.

Gentine, P., Entekhabi, D., Chehbouni, A., Boulet, G. and Duchemin, B.: Analysis of evaporative fraction diurnal behaviour, Agric. For. Meteorol., doi:10.1016/j.agrformet.2006.11.002, 2007.

Gilbert, N.: Water under pressure: a UN analysis sets out global water-management concerns ahead of Earth Summit, Nature, 483(7389), 256–258, 2012.

Guan, K., Wu, J., Anderson, M. C., Kimball, J., Frolking, S., Li, B. and Lobell, D.: The shared and unique value of optical, flourescence, thermal and microwave satellite data for estimating large-scale crop yields (Accpeted), Remote Sens. Environ., 199, 333–349, doi:https://doi.org/10.1016/j.rse.2017.06.043, 2016.

Guanter, L., Zhang, Y., Jung, M., Joiner, J., Voigt, M., Berry, J. A., Frankenberg, C., Huete,

A. R., Zarco-Tejada, P., Lee, J.-E., Moran, M. S., Ponce-Campos, G., Beer, C., Camps-Valls, G., Buchmann, N., Gianelle, D., Klumpp, K., Cescatti, A., Baker, J. M. and Griffis, T. J.: Global and time-resolved monitoring of crop photosynthesis with chlorophyll fluorescence, Proc. Natl. Acad. Sci., doi:10.1073/pnas.1320008111, 2014.

Hassan-Esfahani, L., Torres-Rua, A., Jensen, A. and McKee, M.: Assessment of surface soil moisture using high-resolution multi-spectral imagery and artificial neural networks, Remote Sens., 7(3), 2627–2646, doi:10.3390/rs70302627, 2015.

Hassan-Esfahani, L., Torres-Rua, A., Jensen, A. and Mckee, M.: Spatial Root Zone Soil Water Content Estimation in Agricultural Lands Using Bayesian-Based Artificial Neural Networks and High- Resolution Visual, NIR, and Thermal Imagery, Irrig. Drain., 66(2), 273–288, doi:10.1002/ird.2098, 2017.

Hoffmann, H., Nieto, H., Jensen, R., Guzinski, R., Zarco-Tejada, P. and Friborg, T.: Estimating evaporation with thermal UAV data and two-source energy balance models, Hydrol. Earth Syst. Sci., 20(2), 697–713, doi:10.5194/hess-20-697-2016, 2016.

Houborg, R., Anderson, M. C., Norman, J. M., Wilson, T. and Meyers, T.: Intercomparison of a “bottom-up” and “top-down” modeling paradigm for estimating carbon and energy fluxes over a variety of vegetative regimes across the U.S., Agric. For. Meteorol., 149(12), 2162–2182, doi:10.1016/j.agrformet.2009.10.002, 2009.

Jung, M., Reichstein, M., Margolis, H. A., Cescatti, A., Richardson, A. D., Arain, M. A., Arneth, A., Bernhofer, C., Bonal, D., Chen, J., Gianelle, D., Gobron, N., Kiely, G., Kutsch, W., Lasslop, G., Law, B. E., Lindroth, A., Merbold, L., Montagnani, L., Moors, E. J., Papale, D., Sottocornola, M., Vaccari, F. and Williams, C.: Global patterns of land-atmosphere fluxes of carbon dioxide, latent heat, and sensible heat derived from eddy covariance, satellite, and meteorological observations, J. Geophys. Res. Biogeosciences, 116(3), doi:10.1029/2010JG001566, 2011.

Kljun, N., Calanca, P., Rotach, M. W. and Schmid, H. P.: A simple two-dimensional parameterisation for Flux Footprint Prediction (FFP), Geosci. Model Dev., 8(11), 3695–3713, doi:10.5194/gmd-8-3695-2015, 2015.

Klosterman, S., Melaas, E., Wang, J., Martinez, A., Frederick, S., O’Keefe, J., Orwig, D. A., Wang, Z., Sun, Q., Schaaf, C., Friedl, M. and Richardson, A. D.: Fine-scale perspectives on landscape phenology from unmanned aerial vehicle (UAV) photography, Agric. For. Meteorol., doi:10.1016/j.agrformet.2017.10.015, 2018.

Kustas, W. P. and Norman, J. M.: Evaluation of soil and vegetation heat flux predictions using a simple two-source model with radiometric temperatures for partial canopy cover, Agric. For. Meteorol., 94(1), 13–29, doi:10.1016/S0168-1923(99)00005-2, 1999.

Kustas, W. P., Anderson, M. C., Alfieri, J. G., Knipper, K., Torres-Rua, A., Parry, C. K., Hieto, H., Agam, N., White, A., Gao, F., McKee, L., Prueger, J. H., Hipps, L. E., Los, S., Alsina, M., Sanchez, L., Sams, B., Dokoozlian, N., McKee, M., Jones, S., Yang, Y., Wilson, T. G., Lei, F., McElrone, A., Heitman, J. L., Howard, A. M., Post, K., Melton, F. and Hain, C.: The Grape Remote sensing Atmospheric Profile and Evapotranspiration eXperiment (GRAPEX), Bull. Am. Meteorol. Soc., BAMS-D-16-0244.1, doi:10.1175/BAMS-D-16-0244.1, 2018.

Laliberte, A. S., Goforth, M. A., Steele, C. M. and Rango, A.: Multispectral remote sensing from unmanned aircraft: Image processing workflows and applications for rangeland environments, Remote Sens., 3(11), 2529–2551, doi:10.3390/rs3112529, 2011.

Lawrence, D. M., Oleson, K. W., Flanner, M. G., Thornton, P. E., Swenson, S. C., Lawrence,

P. J., Zeng, X., Yang, Z., Levis, S. and Sakaguchi, K.: Parameterization improvements and functional and structural advances in version 4 of the Community Land Model, J. Adv. Model. Earth Syst., 3(1), 2011.

Li, C. C.: Path Analysis-a primer., The Boxwood Press., 1975.

Lipton, A. E., Liang, P., Jiménez, C., Moncet, J. L., Aires, F., Prigent, C., Lynch, R., Galantowicz, J. F., D'Entremont, R. P. and Uymin, G.: Sources of discrepancies between satellite-derived and land surface model estimates of latent heat fluxes, J. Geophys. Res., 120(6), 2325–2341, doi:10.1002/2014JD022641, 2015.

Mallick, K., Bhattacharya, B. K. and Patel, N. K.: Estimating volumetric surface moisture content for cropped soils using a soil wetness index based on surface temperature and NDVI, Agric. For. Meteorol., 149(8), 1327–1342, doi:10.1016/j.agrformet.2009.03.004, 2009.

Manfreda, S., McCabe, M. F., Miller, P. E., Lucas, R., Madrigal, V. P., Mallinis, G., Dor, E. B., Helman, D., Estes, L., Ciraolo, G., Müllerová, J., Tauro, F., de Lima, M. I., de Lima, J. L. M. P., Maltese, A., Frances, F., Caylor, K., Kohv, M., Perks, M., Ruiz-Pérez, G., Su, Z., Vico, G. and Toth, B.: On the use of unmanned aerial systems for environmental monitoring, Remote Sens., 10(4), 641, doi:10.3390/rs10040641, 2018.

McCabe, M. F., Rodell, M., Alsdorf, D. E., Miralles, D. G., Uijlenhoet, R., Wagner, W., Lucieer, A., Houborg, R., Verhoest, N. E. C., Franz, T. E., Shi, J., Gao, H. and Wood, E. F.: The future of Earth observation in hydrology, Hydrol. Earth Syst. Sci., 21(7), 3879–3914, doi:10.5194/hess-21-3879-2017, 2017.

Metzger, S.: Surface-atmosphere exchange in a box: Making the control volume a suitable representation for in-situ observations, Agric. For. Meteorol., 255, 68–80, doi:10.1016/j.agrformet.2017.08.037, 2018.

Moran, M. S., Clarke, T. R., Inoue, Y. and Vidal, A.: Estimating crop water deficit using the relation between surface-air temperature and spectral vegetation index, Remote Sens. Environ., 49(3), 246–263, doi:10.1016/0034-4257(94)90020-5, 1994.

Moran, M. S., Inoue, Y. and Barnes, E. M.: Opportunities and limitations for image-based remote sensing in precision crop management, Remote Sens. Environ., 61(3), 319–346, doi:10.1016/S0034-4257(97)00045-X, 1997.

Moreno-Martínez, Á., Camps-Valls, G., Kattge, J., Robinson, N., Reichstein, M., van Bodegom, P., Kramer, K., Cornelissen, J. H. C., Reich, P., Bahn, M., Niinemets, Ü., Peñuelas, J., Craine, J. M., Cerabolini, B. E. L., Minden, V., Laughlin, D. C., Sack, L., Allred, B., Baraloto, C., Byun, C., Soudzilovskaia, N. A. and Running, S. W.: A methodology to derive global maps of leaf traits using remote sensing and climate data, Remote Sens. Environ., 218, 69–88, doi:10.1016/j.rse.2018.09.006, 2018.

Morillas, L., Villagarcía, L., Domingo, F., Nieto, H., Uclés, O. and García, M.: Environmental factors affecting the accuracy of surface fluxes from a two-source model in Mediterranean drylands: Upscaling instantaneous to daytime estimates, Agric. For. Meteorol., 189–190, 140–158, doi:10.1016/j.agrformet.2014.01.018, 2014.

Mørup, M.: Applications of tensor (multiway array) factorizations and decompositions in data mining, Wiley Interdiscip. Rev. Data Min. Knowl. Discov., 1(1), 24–40, doi:10.1002/widm.1, 2011.

Nemani, R. R. and Running, S. W.: Estimation of Regional Surface Resistance to Evapotranspiration from NDVI and Thermal-IR AVHRR Data, J. Appl. Meteor, doi:10.1175/1520-0450(1989)028<0276:EORSRT>2.0.CO;2, 1989.

Njoku, E. G., Jackson, T. J., Lakshmi, V., Chan, T. K. and Nghiem, S. V.: Soil moisture retrieval from AMSR-E, IEEE Trans. Geosci. Remote Sens., 41(2 PART 1), 215–228, doi:10.1109/TGRS.2002.808243, 2003.

Noilhan, J. and Planton, S.: A Simple Parameterization of Land Surface Processes for Meteorological Models, Mon. Weather Rev., 117(3), 536–549, doi:10.1175/1520-0493(1989)117<0536:ASPOLS>2.0.CO;2, 1989.

Ortega-Farías, S., Ortega-Salazar, S., Poblete, T., Kilic, A., Allen, R., Poblete-Echeverría, C., Ahumada-Orellana, L., Zuñiga, M. and Sepúlveda, D.: Estimation of energy balance components over a drip-irrigated olive orchard using thermal and multispectral cameras placed on a helicopter-based unmanned aerial vehicle (UAV), Remote Sens., 8(8), 1–18, doi:10.3390/rs8080638, 2016.

P. D. Colaizzi, P. D., S. R. Evett, S. R., T. A. Howell, T. A. and J. A. Tolk, J. A.: Comparison of Five Models to Scale Daily Evapotranspiration from One-Time-of-Day Measurements, Trans. ASABE, doi:10.13031/2013.22056, 2006.

Persson, G.: Willow stand evapotranspiration simulated for Swedish soils, Agric. Water Manag., 28(4), 271–293, doi:10.1016/0378-3774(95)01182-X, 1995.

Phillips, C. J., Marden, M. and Suzanne, L. M.: Observations of root growth of young poplar and willow planting types, New Zeal. J. For. Sci., 44(1), doi:10.1186/s40490-014-0015-6, 2014.

Pilegaard, K., Ibrom, A., Courtney, M. S., Hummelsh??j, P. and Jensen, N. O.: Increasing net CO2 uptake by a Danish beech forest during the period from 1996 to 2009, Agric. For. Meteorol., 151(7), 934–946, doi:10.1016/j.agrformet.2011.02.013, 2011.

Potter, C. S., Randerson, J. T., Field, C. B., Matson, P. A., Vitousek, P. M., Mooney, H. A. and Klooster, S. A.: Terrestrial ecosystem production: A process model based on global satellite and surface data, Global Biogeochem. Cycles, 7(4), 811–841, doi:10.1029/93GB02725, 1993.

Qiu, J., Crow, W. T., Mo, X. and Liu, S.: Impact of Temporal Autocorrelation Mismatch on the Assimilation of Satellite-Derived Surface Soil Moisture Retrievals, , 7(8), 1–9, 2014.

Running, S. W., Baldocchi, D. D., Turner, D. P., Gower, S. T., Bakwin, P. S. and Hibbard, K. A.: A global terrestrial monitoring network integrating tower fluxes, flask sampling, ecosystem modeling and EOS satellite data, Remote Sens. Environ., 70(1), 108–127, doi:10.1016/S0034-4257(99)00061-9, 1999.

Running, S. W., Nemani, R. R., Heinsch, F. A. N. N., Zhao, M., Reeves, M. and Hashimoto, H.: A Continuous Satelite-lDerived Measure of Global Terrestrial Primary Production, Bioscience, 54(6), 547, doi:10.1641/0006-3568(2004)054, 2004.

Sanderson, R.: Introduction to remote sensing, New Mex. State Univ., 25–26, 2010.

Sandholt, I., Rasmussen, K. and Andersen, J.: A simple interpretation of the surface temperature/vegetation index space for assessment of surface moisture status, Remote Sens. Environ., 79(2–3), 213–224, doi:10.1016/S0034-4257(01)00274-7, 2002.

Sims, D. A., Rahman, A. F. and Roberts, D. A.: Use of Hyperspectral Reflectance Indices for Estimation of Gross Carbon Flux and light use Efficiency Crossdiverse Vegetation Types, Int. J. Geoinformatics, 2(1), 2006.

Sivapalan, M., Takeuchi, K., Franks, S. W., Gupta, V. K., Karambiri, H., Lakshmi, V., Liang, X., McDonnell, J. J., Mendiondo, E. M., O'Connell, P. E., Oki, T., Pomeroy, J. W., Schertzer, D., Uhlenbrook, S. and Zehe, E.: IAHS Decade on Predictions in Ungauged Basins (PUB), 2003-2012: Shaping an exciting future for the hydrological sciences, Hydrol. Sci. J., 48(6), 857–880, doi:10.1623/hysj.48.6.857.51421, 2003.

Sobol, I. M.: Global sensitivity indices for nonlinear mathematical models and their Monte Carlo estimates, Math. Comput. Simul., doi:10.1016/S0378-4754(00)00270-6, 2001.

Sobrino, J. A., Franch, B., Mattar, C., Jiménez-Muñoz, J. C. and Corbari, C.: A method to estimate soil moisture from Airborne Hyperspectral Scanner (AHS) and ASTER data: Application to SEN2FLEX and SEN3EXP campaigns, Remote Sens. Environ., 117, 415–428, doi:10.1016/j.rse.2011.10.018, 2012.

Sorooshian, S., Duan, Q. and Gupta, V. K.: Calibration of rainfall- runoff models: Application of global optimization to the Sacramento Soil Moisture Accounting Model, Water Resour. Res., doi:10.1029/92WR02617, 1993.

Stisen, S., Sandholt, I., Nørgaard, A., Fensholt, R. and Eklundh, L.: Estimation of diurnal air temperature using MSG SEVIRI data in West Africa, Remote Sens. Environ., 110(2), 262–274, doi:10.1016/j.rse.2007.02.025, 2007.

Stoy, P. C., Mauder, M., Foken, T., Marcolla, B., Boegh, E., Ibrom, A., Arain, M. A., Arneth, A., Aurela, M., Bernhofer, C., Cescatti, A., Dellwik, E., Duce, P., Gianelle, D., van Gorsel, E., Kiely, G., Knohl, A., Margolis, H., Mccaughey, H., Merbold, L., Montagnani, L., Papale, D., Reichstein, M., Saunders, M., Serrano-Ortiz, P., Sottocornola, M., Spano, D., Vaccari, F. and Varlagin, A.: A data-driven analysis of energy balance closure across FLUXNET research sites: The role of landscape scale heterogeneity, Agric. For. Meteorol., 171–172, 137–152, doi:10.1016/j.agrformet.2012.11.004, 2013.

Sukhdev, P.: Smarter metrics will help fix our food system world-view, Nature, 558(7708), doi:10.1038/d41586-018-05328-1, 2018.

van der Tol, C., Verhoef, W., Timmermans, J., Verhoef, a. and Su, Z.: An integrated model of soil-canopy spectral radiances, photosynthesis, fluorescence, temperature and energy balance, Biogeosciences, 6(12), 3109–3129, doi:10.5194/bg-6-3109-2009, 2009.

Vivoni, E. R.: Spatial patterns, processes and predictions in ecohydrology: Integrating technologies to meet the challenge, Ecohydrology, 5(3), 235–241, doi:10.1002/eco.1248, 2012.

Vivoni, E. R., Rango, A., Anderson, C. A., Pierini, N. A., Schreiner-Mcgraw, A. P., Saripalli, S. and Laliberte, A. S.: Ecohydrology with unmanned aerial vehicles, Ecosphere, 5(10), doi:10.1890/ES14-00217.1, 2014.

Vrugt, J. A., Gupta, H. V., Bastidas, L. A., Bouten, W. and Sorooshian, S.: Effective and efficient algorithm for multiobjective optimization of hydrologic models, Water Resour. Res., doi:10.1029/2002WR001746, 2003.

Wada, Y. and Bierkens, M. F. P.: Sustainability of global water use: Past reconstruction and future projections, Environ. Res. Lett., 9(10), doi:10.1088/1748-9326/9/10/104003, 2014.

Wallace, J. S.: Increasing agricultural water use efficiency to meet future food production, Agric. Ecosyst. Environ., 82(1–3), 105–119, doi:10.1016/S0167-8809(00)00220-6, 2000.

Walter, A., Finger, R., Huber, R. and Buchmann, N.: Opinion: Smart farming is key to developing sustainable agriculture, Proc. Natl. Acad. Sci., 114(24), 6148–6150, doi:10.1073/pnas.1707462114, 2017.

Wang, S., Ibrom, A., Bauer-Gottwein, P. and Garcia, M.: Incorporating diffuse radiation into a light use efficiency and evapotranspiration model: An 11-year study in a high latitude deciduous forest, Agric. For. Meteorol., 248(July), 479–493, doi:10.1016/j.agrformet.2017.10.023, 2018a.

Wang, S., Garcia, M., Ibrom, A., Jakobsen, J., Josef Köppl, C., Mallick, K., Looms, M. and Bauer-Gottwein, P.: Mapping Root-Zone Soil Moisture Using a Temperature–Vegetation Triangle Approach with an Unmanned Aerial System: Incorporating Surface Roughness from Structure from Motion, Remote Sens., 10(12), 1978, 2018b.

Wang, W., Wang, X., Wang, L., Lu, Y., Li, Y. and Sun, X.: Soil moisture estimation for spring wheat in a semiarid area based on low-altitude remote-sensing data collected by small-sized unmanned aerial vehicles, J. Appl. Remote Sens., 12(2), 22207, 2018c.

Westoby, M. J., Brasington, J., Glasser, N. F., Hambrey, M. J. and Reynolds, J. M.: “Structure-from-Motion” photogrammetry: A low-cost, effective tool for geoscience applications, Geomorphology, 179, 300–314, doi:10.1016/j.geomorph.2012.08.021, 2012.

Wood, E. F., Roundy, J. K., Troy, T. J., van Beek, L. P. H., Bierkens, M. F. P., Blyth, E., de Roo, A., Döll, P., Ek, M., Famiglietti, J., Gochis, D., van de Giesen, N., Houser, P., Jaffé, P. R., Kollet, S., Lehner, B., Lettenmaier, D. P., Peters-Lidard, C., Sivapalan, M., Sheffield, J., Wade, A. and Whitehead, P.: Hyperresolution global land surface modeling: Meeting a grand challenge for monitoring Earth’s terrestrial water, Water Resour. Res., 47(5), W05301, doi:10.1029/2010WR010090, 2011.

Wu, J., Linden, L. van der, Lasslop, G., Carvalhais, N., Pilegaard, K., Beier, C. and Ibrom, A.: Effects of climate variability and functional changes on the interannual variation of the carbon balance in a temperate deciduous forest., 2012.

Xu, K., Metzger, S. and Desai, A. R.: Upscaling tower-observed turbulent exchange at fine spatio-temporal resolution using environmental response functions, Agric. For. Meteorol., 232, 10–22, doi:10.1016/j.agrformet.2016.07.019, 2017.

Yapo, P. O., Gupta, H. V. and Sorooshian, S.: Multi-objective global optimization for hydrologic models, J. Hydrol., doi:10.1016/S0022-1694(97)00107-8, 1998.

Zarco-Tejada, P. J., González-Dugo, V. and Berni, J. A. J.: Fluorescence, temperature and narrow-band indices acquired from a UAV platform for water stress detection using a micro-hyperspectral imager and a thermal camera, Remote Sens. Environ., 117, 322–337, doi:10.1016/j.rse.2011.10.007, 2012.

Zarco-Tejada, P. J., Morales, A., Testi, L. and Villalobos, F. J.: Spatio-temporal patterns of chlorophyll fluorescence and physiological and structural indices acquired from hyperspectral imagery as compared with carbon fluxes measured with eddy covariance, Remote Sens. Environ., 133, 102–115, doi:10.1016/j.rse.2013.02.003, 2013.

Zarco-Tejada, P. J., Diaz-Varela, R., Angileri, V. and Loudjani, P.: Tree height quantification using very high resolution imagery acquired from an unmanned aerial vehicle (UAV) and automatic 3D photo-reconstruction methods, Eur. J. Agron., 55, 89–99, doi:10.1016/j.eja.2014.01.004, 2014.

Zarco-Tejada, P. J., Camino, C., Beck, P. S. A., Calderon, R., Hornero, A., Hernández-Clemente, R., Kattenborn, T., Montes-Borrego, M., Susca, L., Morelli, M., Gonzalez-Dugo, V., North, P. R. J., Landa, B. B., Boscia, D., Saponari, M. and Navas-Cortes, J. A.: Previsual symptoms of Xylella fastidiosa infection revealed in spectral plant-trait alterations, Nat. Plants, 4(7), 432–439, doi:10.1038/s41477-018-0189-7, 2018.

Zhang, L., Potter, N., Hickel, K., Zhang, Y. and Shao, Q.: Water balance modeling over variable time scales based on the Budyko framework - Model development and testing, J. Hydrol., doi:10.1016/j.jhydrol.2008.07.021, 2008.

9 Papers

I **Wang**, **S.**, Baum, A., Zarco-Tejada, P., Dam-Hansen, C., Thorseth, A., Bauer-Gottwein P., Bandini F., & Garcia M. (2018) "Unmanned Aerial System multispectral mapping for low and variable solar irradiance conditions: potential of tensor decomposition". *Submitted.*

II **Wang, S**., Ibrom, A., Bauer-Gottwein, P., & Garcia, M. (2018). "Incorporating diffuse radiation into a light use efficiency and evapotranspiration model: An 11-year study in a high latitude deciduous forest". *Agricultural and Forest Meteorology*, 248, 479-493.

III **Wang**, **S.**, Garcia, M., Ibrom, A., Jakobsen, J., Josef Köppl, C., Mallick, K., Looms, M., & Bauer-Gottwein, P. (2018) "Mapping root zone soil moisture using a temperature-vegetation triangle approach with an Unmanned Aerial System: incorporating surface roughness from Structure-from-Motion". *Remote Sensing*, 10 (12), 1978.

IV **Wang**, **S.**, Garcia, M., Bauer-Gottwein, P., Jakobsen, J., Zarco-Tejada, P., Bandini, F., Sobejano Paz, V., & Ibrom, A. (2018) "High spatial resolution monitoring land surface energy, water and CO_2 fluxes from an unmanned aerial system". *Under review.*

V **Wang**, **S.**, Garcia, M., Ibrom, A., & Bauer-Gottwein, P. (2018) "Interpolating rapidly changing land surface energy, water and CO_2 fluxes between remote sensing acquisitions from an Unmanned Aerial System". *Manuscript.*

TEXT FOR WWW-VERSION (with out papers)

In this online version of the thesis, **paper I-V** are not included but can be obtained from electronic article databases e.g. via www.orbit.dtu.dk or on request from.

DTU Environment
Technical University of Denmark
Miljoevej, Building 113
2800 Kgs. Lyngby
Denmark

info@env.dtu.dk.

The Department of Environmental Engineering (DTU Environment) conducts science-based engineering research within five sections: Air, Land & Water Resources, Urban Water Systems, Water Technology, Residual Resource Engineering, Environmental Fate and Effect of Chemicals.

The department dates back to 1865, when Ludvig August Colding gave the first lecture on sanitary engineering as response to the cholera epidemics in Copenhagen in the late 1800s.

Department of Environmental Engineering
Technical University of Denmark

DTU Environment
Bygningstorvet, Building 115
2800 Kgs. Lyngby
Tlf. +45 4525 1600
Fax +45 4593 2850

www.env.dtu.dk